

Particle MCMC with Poisson Resampling: Parallelization and Continuous Time Models

T. Cakala, B. Miasojedow, W. Niemiro

February 15, 2022

Abstract

We introduce a new version of particle filter in which the number of “children” of a particle at a given time has a Poisson distribution. As a result, the number of particles is random and varies with time. An advantage of this scheme is that descendants of different particles can evolve independently. It makes easy to parallelize computations. Moreover, particle filter with Poisson resampling is readily adapted to the case when a hidden process is a continuous time, piecewise deterministic semi-Markov process. We show that the basic techniques of particle MCMC, namely particle independent Metropolis-Hastings, particle Gibbs Sampler and its version with ancestor sampling, work under our Poisson resampling scheme. Our version of particle Gibbs Sampler is uniformly ergodic under the same assumptions as its standard counterpart. We present simulation results which indicate that our algorithms can compete with the existing methods.

KEYWORDS: Sequential Monte Carlo, Particle Markov chain Monte Carlo, Parallel computations, Poisson distribution, Hidden Markov model, Piecewise deterministic semi-Markov process, Pseudo-marginal, Independent Metropolis-Hastings Algorithm, Gibbs Sampler, Ancestor Sampling.

1 Introduction

Particle Filters (PF) and more generally Sequential Monte Carlo methods (SMC) ([Gordon et al., 1993](#); [Doucet et al., 2001](#); [Moral et al., 2006](#)) are general framework for statistical inference for state space models. SMC methods have proven effective in various scenarios covering: object tracking, time series analysis in non-Gaussian models ([Gordon et al., 1993](#); [Doucet et al., 2001](#)), graphical models ([Naesseth et al., 2014](#)), rare events estimation ([C  rou et al., 2011](#)), phylogenetic inference ([Bouchard-C  t   et al., 2012](#)) and model selection ([Schfer and Chopin, 2011](#)). The seminal paper ([Andrieu et al., 2010](#)) introduced Particle Markov Chain Monte Carlo methods (PMCMC), which combine strengths of MCMC and SMC algorithms.

Most of the research on SMC methods and their extensions is focused on discrete time models. Statistical inference for continuous time models is usually performed via discretisation of time, see for example ([Golightly and Wilkinson, 2011](#)) and by introducing rather complex birth-death moves ([Finke et al., 2014](#)). The main difficulty in designing SMC methods for continuous time models is the fact that the standard resampling step requires synchronisation of all the paths. In the current paper we introduce a unified approach for both discrete and continuous time setting. We propose a new Poisson resampling scheme. Rather surprisingly, this scheme allows for a straightforward extension of PMCMC to a wide class of piecewise deterministic processes (PDP). They are processes which evolve deterministically in continuous time except for a countable collection of stopping times at which they randomly jump, see ([Davis, 1984](#)). PDPs have recently attracted

much attention because they are most natural models of a lot of phenomena in biology (Rudnicki and Tyran-Kamińska, 2017) and in other branches of science.

In addition, the standard resampling scheme is challenging to implement in parallel, see for example (Paige et al., 2014a; Murray et al., 2016). Our scheme is much easier to parallelise, due to the fact that only partial synchronisation is required in Poisson resampling. Our algorithm PTPF (Poisson Tree PF), similarly to (Paige et al., 2014a) generates a branching process. The main advantage of our approach, and the difference from (Paige et al., 2014a), is that PTPF can be directly used within PMCMC methods. Moreover, our framework allows us to perform ancestor sampling in the particle Gibbs algorithm in the spirit of (Lindsten et al., 2014). We prove that our version of Particle Gibbs Sampler (in the discrete time setting) is uniformly ergodic, under the same assumptions as its standard counterpart (Lindsten et al., 2015).

Since the Poisson resampling produces a random (and varying) number of particles, it is essential to control their population size. To make our algorithms practically applicable, we have to introduce some sort of synchronisation of particles. (Even though synchronisation is *not* necessary to ensure convergence to the target.) The inherently parallel structure of Poisson resampling has to be reconciled with (partial) synchronisation. This is relatively easy for discrete time models and much harder for continuous time models. Nonetheless, we have designed some rules (recipes for choosing control parameters in PTPF) which keep the population of particles approximately constant.

Apart from theoretical considerations, we demonstrate our method on a few challenging examples. Our simulations indicate that in the discrete time setting our algorithms yield results as good as standard PMCMC. Parallel implementation of our algorithms leads to significant gains in efficiency. For continuous time models our algorithms can compete with the existing methods, and in some examples outperform them.

The paper is organised as follows. In Section 2 we introduce a general class of semi-Markov state space models including discrete time state space models and piece-wise deterministic hidden Markov processes. Next in the Section 3 we present our basic Particle Filter (PTPF). In Section 4 we show how to construct PMCMC methods based on PTPF. In Section 5 we introduce specific rules designed to control the size of the population of particles and we define our version of ancestor resampling. Finally, in Section 6 we present numerical simulations.

2 Semi-Markov State-Space Models

We consider a rather general family of state-space semi-Markov models. We first consider continuous time models. Assume that $\{\Xi(t), t \geq t_{\min}\}$ is a *piece-wise deterministic process* with values in a Polish space \mathcal{X} and with càdlàg trajectories. The process jumps randomly at a countable set of random times $T_1 < \dots < T_k < \dots$. Between jumps it evolves according to a deterministic law. We consider a finite time horizon t_{\max} and write $M = \min\{k : T_k > t_{\max}\}$. Assume that process $\Xi = \{\Xi(t), t_{\min} \leq t \leq t_{\max}\}$ is uniquely determined by its space-time *skeleton* $(X_{1:M}, T_{1:M})$, where

$$(2.1) \quad X_k = \Xi(T_k-), \quad k = 1, \dots, M.$$

Note that our definition of the skeleton is different from the standard one, e.g. in Davis (1984), and perhaps less intuitive. We require that the trajectory of Ξ in the time interval $[T_{k-1}, T_k[$ depends deterministically on its value at the *end* of the interval. (We define the skeleton via (2.1) to facilitate our construction of ancestor sampling in Section 5.) We assume that random variable M is almost surely finite. Our basic assumption is that the skeleton is Markovian, governed by a space-time stochastic transition kernel K . The

(prior) probability distribution of the skeleton can be written in a concise form

$$(2.2) \quad \begin{aligned} \pi_{\text{prior}}(\mathrm{d}x_{1:m}, \mathrm{d}t_{1:m}) &= \mathbb{P}(X_1 \in \mathrm{d}x_1, T_1 \in \mathrm{d}t_1, \dots, X_m \in \mathrm{d}x_m, T_m \in \mathrm{d}t_m) \\ &= \prod_{k=1}^m K(x_{k-1}, t_{k-1}; \mathrm{d}x_k, \mathrm{d}t_k), \end{aligned}$$

if we adopt a convention explained below. The initial distribution is written as $\mathbb{P}(X_1 \in \mathrm{d}x_1, T_1 \in \mathrm{d}t_1) = K(x_0, t_0; \mathrm{d}x_1, \mathrm{d}t_1)$, where (x_0, t_0) is a fictitious state with $t_0 = t_{\min}$. Note also that the last point of the skeleton (x_m, t_m) falls beyond the time horizon ($t_m > t_{\max}$). In the sequel, ξ denotes a sample path of Ξ and we write $\xi_{[t', t'']} = \{\xi(t), t \leq t' < t''\}$. Some more details and an explicit construction of Ξ are in the Supplementary Material.

The setup described above encompasses continuous time *piece-wise deterministic Markov processes* (Davis, 1984), in particular pure jump Markov processes, and a wide class of piece-wise deterministic non-Markovian processes (Whiteley et al., 2011; Finke et al., 2014).

The process Ξ is hidden and thus (2.2) plays the role of the prior. Let Υ be an observed random element which depends on Ξ . The *target probability distribution* is the posterior of Ξ given $\Upsilon = y$. Since y is fixed, it will not be explicitly indicated. We only need to assume that we have a family of likelihood functions $\ell(\xi_{[t, t']})$ which satisfy the condition

$$(2.3) \quad \ell(\xi_{[t, t'']}) = \ell(\xi_{[t, t']})\ell(\xi_{[t', t'']}),$$

for $t < t' < t''$. (By convention, $\ell(\xi_{[t, t']})$ is understood as $\ell(\xi_{[t, t_{\max}]})$ whenever $t' > t_{\max}$.) In most applications the likelihoods satisfy (2.3). First typical example is when $\Upsilon = (Y_1, \dots, Y_p)$ is just a sequence of “noisy measurements” on ξ at discrete “observation times”, say $t_{\min} \leq t_{\text{obs}}^1 < \dots < t_{\text{obs}}^p \leq t_{\max}$. We assume that Y_r depends only on $\xi(t_{\text{obs}}^r)$ and $\ell(\xi_{[t, t']})$ corresponds to $\{y_r : t_{\text{obs}}^r \in [t, t']\}$. The second example is when Υ a fully observed continuous time random process $\{\Upsilon(t) : t_{\min} \leq t \leq t_{\max}\}$ and $\ell(\xi_{[t, t']})$ corresponds to $y_{[t, t']}$.

Recall that $\xi_{[t_{\min}, t_{\max}]}$ is represented by its skeleton $(x_{1:m}, t_{1:m})$. Since the trajectory $\xi_{[t_{k-1}, t_k]}$ depends deterministically on $\xi(t_k-) = x_k$, we can write $\ell(\xi_{[t_{k-1}, t_k]}) = \ell(x_k; t_{k-1}, t_k)$. The posterior distribution of $(X_{1:M}, T_{1:M})$ is given by

$$(2.4) \quad \pi_{\text{post}}(\mathrm{d}x_{1:m}, \mathrm{d}t_{1:m}) = \frac{1}{z} \cdot \prod_{k=1}^m K(x_{k-1}, t_{k-1}; \mathrm{d}x_k, \mathrm{d}t_k) \ell(x_k; t_{k-1}, t_k),$$

where z is a norming constant (the integral of the likelihood with respect to the prior). Our main objects of interest are z and the posterior $\pi = \pi_{\text{post}}$. From now on, we most often drop the subscript ‘post’.

Discrete time hidden Markov models fit in our setup as a special case (identified with piece-wise constant processes). Let $\Xi = (X_1, \dots, X_m)$ be a discrete time Markov chain (in general, inhomogeneous in time) with one-step transition kernels P_1, \dots, P_{m-1} . Using a convention explained earlier, the joint (prior) probability distribution is

$$\pi_{\text{prior}}(\mathrm{d}x_{1:m}) = \mathbb{P}(X_1 \in \mathrm{d}x_1, \dots, X_m \in \mathrm{d}x_m) = \prod_{t=1}^m P_{t-1}(x_{t-1}, \mathrm{d}x_t).$$

The natural assumption about the process of observations in the discrete time setting is that $\Upsilon = (Y_1, \dots, Y_m)$, where Y_t depends only on *one* state X_t of the Markov chain. The likelihood is of the form $\ell_t(x_t)$ and consequently,

$$(2.5) \quad \pi_{\text{post}}(\mathrm{d}x_{1:m}) = \frac{1}{z} \cdot \prod_{t=1}^m P_{t-1}(x_{t-1}, \mathrm{d}x_t) \ell_t(x_t).$$

3 Poisson Tree Particle Filter

To define *Poisson Tree Particle Filter* (PTPF) and particle MCMC algorithms based on PTPF we introduce suitable notations. PTPF produces a random structure $\mathbb{A} = (\mathcal{V}, \mathcal{E}, \mathbf{X}, \mathbf{T}, S)$.

- $(\mathcal{V}, \mathcal{E})$ is a directed graph with the set \mathcal{V} of nodes and set \mathcal{E} of edges (arrows).
- $\mathbf{X} = \{X_i : i \in \mathcal{V}\}$ is a collection of random variables with values in \mathcal{X} .
- $\mathbf{T} = \{T_i : i \in \mathcal{V}\}$ is a collection of random variables with values in $[t_{\min}, \infty[$.
- $S \in \mathcal{V}$ is a (random) node identifying a selected path in the graph.

We will also consider two collections of random variables $\mathbf{\Lambda} = \{\Lambda_i : i \in \mathcal{V}\}$ and $\mathbf{W} = \{W_i : i \in \mathcal{V}\}$, which are functions of \mathbb{A} (and of the fixed observation $\Upsilon = y$).

Graph $(\mathcal{V}, \mathcal{E})$ is a directed forest. Every node has at most one incoming edge. A generic element of \mathcal{V} is denoted by i and a generic element of \mathcal{E} by $i \rightarrow j$. If $i \rightarrow j$ then we write $i = \text{pa}(j)$ and $j \in \text{ch}(i)$. It is convenient to add a fictitious node 0 to \mathcal{V} and treat the graph as a tree with root 0, adding arrows $0 \rightarrow i$ for all nodes i with $\text{pa}(i) = \emptyset$. For any $i \in \mathcal{V}$ there is a unique ancestry line denoted by $\text{an}(i)$. It is a sequence of nodes $(a_1(i), \dots, a_k(i))$ such that $a_k(i) = i$, $a_r(i) = \text{pa}(a_{r+1}(i))$ for $r = 1, \dots, k-1$ and $\text{pa}(a_1(i)) = 0$ (note that $\text{an}(i)$ includes i and does not include the artificial root 0). We also write $X_{\text{an}(i)} = (X_{a_1(i)}, \dots, X_{a_k(i)})$ and $T_{\text{an}(i)} = (T_{a_1(i)}, \dots, T_{a_k(i)})$. To every $i \in \mathcal{V}$ there corresponds a sample path of continuous time process $\Xi_i = \{\Xi_i(t) : t_{\min} \leq t < T_i\}$ determined by the space-time skeleton $(X_{\text{an}(i)}, T_{\text{an}(i)})$ (note that Ξ_i is defined on the right open interval $[t_{\min}, T_i[$ and $X_i = \Xi(T_i-)$, in accordance with the conventions introduced in the previous section).

We first describe PTPF informally and explain the role played by all the involved variables. Let us think that node i (or equivalently edge $\text{pa}(i) \rightarrow i$) is an identifier of a “particle” which is born at time $T_{\text{pa}(i)}$. Particle i evolves deterministically from its initial location till time T_i and X_i denotes its location immediately prior to T_i . If $T_i > t_{\max}$ then we say i is a terminal node, $i \in \mathcal{V}_{\text{end}}$. Otherwise, i gives birth to a set $\text{ch}(i)$ of children. This is done as follows. First we choose an “intensity parameter” Λ_i (see the paragraph below). We compute the weight W_i equal to $\ell(X_i; T_{\text{pa}(i)}, T_i)$, i.e. the likelihood corresponding to the deterministic part of trajectory in the interval $[T_{\text{pa}(i)}, T_i[$. Then we sample $N_i \sim \text{Pois}(\Lambda_i W_i)$ and create a set $\text{ch}(i)$ of cardinality N_i (possibly empty) with arrows from i to all $j \in \text{ch}(i)$. For every child $j \in \text{ch}(i)$ we independently sample random pair (X_j, T_j) from the probability distribution $K(X_i, T_i; \cdot, \cdot)$. Every child $j \in \text{ch}(i)$ immediately jumps to its initial location and evolves deterministically till time T_j . This procedure is repeated until no “active” nodes are left. A node i is said to be active, $i \in \mathcal{V}_{\text{act}}$, if $T_i \leq t_{\max}$ and it has not yet undergone the “propagation procedure” described above. The last stage of PTPF is selecting one node S among nodes i which satisfy $T_i > t_{\max}$. The ancestry line $\text{an}(S)$ identifies a sample path of the hidden process $\{\Xi(t), t \in [t_{\min}, t_{\max}]\}$ which is used as an update in pMCMC algorithms. We also compute an estimate \hat{Z} of the norming constant z .

A few more notations are needed to define PTPF more precisely. Assume that for any active node i , the corresponding intensity parameter Λ_i can depend on the history of the whole process before the current time T_i . To avoid vicious circle, at every stage we can pick up (for “propagation”) an active node i with the least T_i . (This last rule is introduced to simplify presentation. Later, in Section 5, it will be relaxed.) History up to time T_i , denoted $\mathcal{H}(T_i)$, is defined as a subtree which includes nodes l, j and arrows $l \rightarrow j$ such that $T_l < T_i$, together with the corresponding variables X_l, X_j, T_l, T_j (let us remember that X_j determines the location of a particle born at moment T_l). In other words, $\mathcal{H}(T_i)$ contains information about all the particles j born before T_i and allows us to compute the likelihoods $\ell(\Xi_{j[t', t'']})$ for $t_{\min} \leq t' < t'' \leq T_j$. Every parameter Λ_i is a function of the history, say $\Lambda_i = \mathbb{L}(\mathcal{H}(T_i))$. Some concrete forms of function \mathbb{L} will be

discussed in Section 5. The initial Λ_0 is equal to a constant λ_0 chosen *a priori*. A pseudo-code defining PTPF is the following.

Algorithm PTPF (Poisson Tree Particle Filter)

```

{ Initialize: }
 $\mathcal{V} := \mathcal{V}_{\text{act}} := \{0\}; \mathcal{E} := \emptyset; \mathcal{V}_{\text{end}} := \emptyset; T_0 := t_0; C_0 := \Lambda_0 := \lambda_0; W_0 := 1$ 
{ Main loop: }
while  $\mathcal{V}_{\text{act}} \neq \emptyset$  do
  Choose  $i \in \mathcal{V}_{\text{act}}$  with minimum  $T_i$  {This requirement will be relaxed}
  if  $i \neq 0$  then
    Compute  $\Lambda_i := \mathbb{L}(\mathcal{H}(T_i))$  {This step will be precised later}
     $C_i := C_{\text{pa}(i)} \Lambda_i$ 
  end if
  Sample  $N_i \sim \text{Pois}(\Lambda_i W_i)$ 
  if  $N_i > 0$  then
    Create set  $\text{ch}(i)$  of cardinality  $N_i$ 
     $\mathcal{V} := \mathcal{V} \cup \text{ch}(i), \mathcal{E} := \mathcal{E} \cup \{i \rightarrow j : j \in \text{ch}(i)\}$ 
    for all  $j \in \text{ch}(i)$  do
      Sample  $(X_j, T_j) \sim K(X_i, T_i; \cdot, \cdot)$  {Propagate}
      Compute  $W_j := \ell(X_j; T_i, T_j)$  {Weigh}
      if  $T_j > t_{\text{max}}$  then
         $\mathcal{V}_{\text{end}} := \mathcal{V}_{\text{end}} \cup \{j\}$ 
      else
         $\mathcal{V}_{\text{act}} := \mathcal{V}_{\text{act}} \cup \{j\}$ 
      end if
    end for
  end if
   $\mathcal{V}_{\text{act}} := \mathcal{V}_{\text{act}} \setminus \{i\}$ 
end while
{ Select S: }
if  $\mathcal{V}_{\text{end}} \neq \emptyset$  then
   $\hat{Z} := \sum_{i \in \mathcal{V}_{\text{end}}} W_i / C_{\text{pa}(i)}$ 
  Select  $S \in \mathcal{V}_{\text{end}}$  from the probability distribution  $\mathbb{P}(S = s) \propto W_s / C_{\text{pa}(s)}$ 
else
   $\hat{Z} := 0$ 
end if
Output  $\hat{Z}, (X_{\text{an}(S)}, T_{\text{an}(S)})$  { Optionally  $\mathbb{A} = (\mathcal{V}, \mathcal{E}, \mathbf{X}, \mathbf{T}, S)$  }

```

For discrete time models, with $\Xi = (X_1, \dots, X_m)$ a few details in PTPF become simpler. We can omit $T_{1:m}$ in the input/output. The tree produced by the algorithm is uniquely represented by $(\mathcal{V}, \mathcal{E}, \mathbf{X}, S)$. Kernel $K(x_i, t_i, dx_j, dt_j)$ is reduced to $P_{t-1}(x_i, dx_j)$, where $t_i = t - 1$ and $t_j = t$. The set of nodes is partitioned into “generations” $\mathcal{V}_t = \{i \in \mathcal{V} : T_i = t\}$, $t = 1, \dots, m$. Nodes belonging to \mathcal{V}_t propagate simultaneously and independently. The set of terminal nodes is $\mathcal{V}_{\text{end}} = \mathcal{V}_m$.

Extended probability distributions

The joint probability distribution of all the random variables in

$$\mathbb{A} = (\mathcal{V}, \mathcal{E}, \mathbf{X}, \mathbf{T}, S)$$

is called the *extended proposal*, following the terminology established in the SMC literature. The extended proposal is denoted by $\psi(\mathcal{V}, \mathcal{E}, d\mathbf{x}, d\mathbf{t}, s)$. Values of random variables X_i , T_i and S are denoted by the corresponding small case letters x_i , t_i and s . Analogously, notations λ_i , w_i and \hat{z} will be used for values of random variables Λ_i , W_i and \hat{Z} , which are functions of $(\mathcal{V}, \mathcal{E}, \mathbf{X}, \mathbf{T})$. Consequently, in the formulae below we use the following notations.

$$w_0 = 1, \quad w_i = \ell(x_i; t_{\text{pa}(i)}, t_i), \quad \lambda_i = \mathbb{L}(\mathcal{H}(t_i)),$$

$$\mathcal{V}_{\text{end}} = \{j \in \mathcal{V} : t_j > t_{\text{max}}\}, \quad c_j = \lambda_0 \prod_{i \in \text{an}(j)} \lambda_i.$$

3.1 REMARK (Equivalence classes). The labels given to nodes of the graph $(\mathcal{V}, \mathcal{E})$ are irrelevant to the behaviour of the algorithm. Strictly speaking, we are interested in the *equivalence classes* $[\mathbb{A}] = [(\mathcal{V}, \mathcal{E}, \mathbf{X}, \mathbf{T}, S)]$, where two structures are equivalent if they differ from each other only by labelling of the nodes. (That is, if there is a one-to-one correspondence between the sets of nodes which preserves the set of arrows, the variables X_i , T_i and S .) In a single “propagation” step of PTPF, node i “produces” n_i children with probability

$$\exp[-\lambda_i w_i] \frac{(\lambda_i w_i)^{n_i}}{n_i!}.$$

A child with label j is then assigned a pair (x_j, t_j) drawn from K . There are $n_i!$ equivalent configurations of children. Therefore, if we consider the distribution of the equivalence class, then the factorial in the Poisson probability cancels out. Let us introduce the following convention. From now on, *we work with the equivalence classes* without making explicit the distinction between a class $[\mathbb{A}]$ and its representative \mathbb{A} .

Now we are in a position to write a formula for the extended proposal. It is convenient to discern two stages: first the marginal distribution of all the variables except S , and then the conditional distribution of S given the rest. This exactly corresponds to the two stages of PTPF: in the “Main loop” we sample $(\mathcal{V}, \mathcal{E}, \mathbf{X}, \mathbf{T})$ and the last part of the algorithm is “Selecting S ”.

The *extended proposal* is given by

$$(3.2) \quad \psi(\mathcal{V}, \mathcal{E}, d\mathbf{x}, d\mathbf{t}) = \prod_{i \in \mathcal{V} \setminus \mathcal{V}_{\text{end}}} \exp[-\lambda_i w_i] (\lambda_i w_i)^{|\text{ch}(i)|} \prod_{j \in \text{ch}(i)} K(x_i, t_i; dx_j, dt_j);$$

$$\psi(\mathcal{V}, \mathcal{E}, d\mathbf{x}, d\mathbf{t}, s) = \psi(\mathcal{V}, \mathcal{E}, d\mathbf{x}, d\mathbf{t}) \frac{w_s / c_{\text{pa}(s)}}{\hat{z}},$$

where

$$\hat{z} = \sum_{i \in \mathcal{V}_{\text{end}}} w_i / c_{\text{pa}(i)}.$$

In (3.2) and everywhere else we use the convention that $\prod_{i \in \emptyset} \dots = 1$. If $\mathcal{V}_{\text{end}} = \emptyset$ then s is undefined.

The *extended target* is concentrated on trees with $\mathcal{V}_{\text{end}} \neq \emptyset$ and is given by

$$(3.3) \quad \phi(\mathcal{V}, \mathcal{E}, d\mathbf{x}, d\mathbf{t}, s) = \psi(\mathcal{V}, \mathcal{E}, d\mathbf{x}, d\mathbf{t}, s) \frac{\hat{z}}{z}$$

$$= \pi(dx_{\text{an}(s)}, dt_{\text{an}(s)}) \cdot \psi_{\text{cond}}(\mathcal{V}, \mathcal{E}, d\mathbf{x}, d\mathbf{t}, s | x_{\text{an}(s)}, t_{\text{an}(s)}),$$

where the *conditional proposal distribution* is

$$(3.4) \quad \psi_{\text{cond}}(\mathcal{V}, \mathcal{E}, d\mathbf{x}, d\mathbf{t}, s | x_{\text{an}(s)}, t_{\text{an}(s)})$$

$$= \prod_{i \in \mathcal{V} \setminus \mathcal{V}_{\text{end}} \setminus \text{an}(s)} \exp[-\lambda_i w_i] (\lambda_i w_i)^{|\text{ch}(i)|} \prod_{j \in \text{ch}(i)} K(x_i, t_i; dx_j, dt_j)$$

$$\times \prod_{i \in \text{an}(s) \setminus \{s\}} \exp[-\lambda_i w_i] (\lambda_i w_i)^{|\text{ch}(i)|-1} \prod_{j \in \text{ch}(i) \setminus \text{an}(s)} K(x_i, t_i; dx_j, dt_j).$$

Formula (3.3) plays a crucial role in our paper. It relates the result of running PTPF (extended proposal ψ) to the extended target ϕ . Thus ϕ is a probability distribution which, when marginalized to the selected path, yields the target distribution π . It is worth mentioning that (3.3) is an exact analogue of a fact established for filters with deterministic number of particles in (Andrieu et al., 2010, see the sentence which follows Theorem 2). Rather unexpectedly, the same relation is true for PTPF.

To verify that equations (3.3) and (3.4) are correct, it is enough to rearrange terms in $\psi(\mathcal{V}, \mathcal{E}, d\mathbf{x}, d\mathbf{t}, s)\hat{z}/z$. By (2.4), if we gather the terms corresponding to the selected path then we obtain

$$\prod_{j \in \text{an}(s)} K(x_{\text{pa}(j)}, t_{\text{pa}(j)}; dx_j, dt_j) w_j / z = \pi(dx_{\text{an}(s)}, dt_{\text{an}(s)}).$$

Note that the product on the LHS includes w_s . Now consider the remaining terms. If $i \in \text{an}(s) \setminus \{s\}$ then the exponent in the expression $(\lambda_i w_i)^{|\text{ch}(i)|-1}$ is decreased by one, because one w_i is included in $\pi(x_{\text{an}(s)}, t_{\text{an}(s)})$ and one λ_i is present in $c_{\text{pa}(s)}$. In the product of $K(x_i, t_i; dx_j, dt_j)$ over the children of i , we drop one term, which corresponds to $j \in \text{an}(s)$, because it is included in $\pi(x_{\text{an}(s)}, t_{\text{an}(s)})$. Thus we see that ψ_{cond} in (3.3) is indeed given by (3.4).

Now we can define the conditional PTPF (cPTPF), i.e. the algorithm which produces a configuration with the probability distribution ψ_{cond} . cPTPF differs from the basic PTPF only in that the conditioning path $(X_{\text{an}(s)}, T_{\text{an}(s)})$ is fixed at the beginning and equal to a given $(X_{1:M}, T_{1:M})$.

Algorithm cPTPF (conditional PTPF)

```

Input  $(X_{1:M}, T_{1:M})$ 
{ Initialize: }
 $\mathcal{V} := \mathcal{V}_{\text{act}} := \{0\} \cup \{1 : M - 1\}$ ;  $\mathcal{E} := \{k - 1 \rightarrow k, k \in \{1 : M\}\}$ 
{ The values  $(X_{1:M}, T_{1:M})$  are inherited from the input and kept fixed }
 $T_0 := t_0$ ;  $C_0 := \Lambda_0 := \lambda_0$ ;  $W_0 := 1$ 
{ Main loop: }
..... { the same as in PTPF }
 $S := M$  {  $S$  identifies the conditioning path }
Output  $(\mathcal{V}, \mathcal{E}, \mathbf{X}, \mathbf{T})$  { Tree with the conditional distribution  $\psi_{\text{cond}}$  }

```

A few comments are due here. In the pseudo-code above, we include the conditioning path $(X_{1:M}, T_{1:M})$ in the tree with labels $\{1 : M\}$ given to the nodes of this path. Remember that labelling of nodes is arbitrary. The only restriction is that in the “Main loop”, newly created nodes are given unique labels (different from $\{1 : M\}$). At the last stage of cPTPF, we set “ $S := M$ ” only to ensure that $(X_{1:M}, T_{1:M}) = (X_{\text{an}(s)}, T_{\text{an}(s)})$, in agreement with our notation in (3.3) and (3.4).

4 Particle MCMC based on PTPF

The two main Particle MCMC algorithms are *Particle Independent Metropolis-Hastings* and *Particle Gibbs Sampler*. Their versions with Poisson resampling are algorithms PTMH and PTGS defined below (PT stands for *Poisson Tree*). We will describe two recipes for simulating a Markov chain $\Xi^{(0)}, \Xi^{(1)}, \dots, \Xi^{(n)}, \dots$, where $\Xi^{(n)} = \{\Xi^{(n)}(t) : t_{\min} \leq t \leq t_{\max}\}$ such that the stationary distribution is the target, i.e. the posterior of hidden Ξ given $\Upsilon = y$. As usual, the trajectories are represented by their skeletons, so we actually simulate sequences $(X^{(n)}, T^{(n)}) = (X_{1:M}^{(n)}, T_{1:M}^{(n)})$, $n = 0, 1, \dots$. The rules of transition from $X = X^{(n)}$ to $X' = X^{(n+1)}$ are the following.

One step of PTMH (Poisson Tree Metropolis-Hastings)

```

Input  $\hat{Z}, (X_{1:M}, T_{1:M})$  { Output of the previous step }
Run PFPP to obtain  $(X_{1:M}^*, T_{1:M}^*)$  and  $\hat{Z}^*$  { Proposal }
Sample  $U \sim U(0, 1)$ 
if  $U < \hat{Z}^*/\hat{Z}$  then
     $(X'_{1:M}, T'_{1:M}) := (X_{1:M}^*, T_{1:M}^*)$ ;  $\hat{Z}' := \hat{Z}^*$  { Accept }
else
     $(X'_{1:M}, T'_{1:M}) := (X_{1:M}, T_{1:M})$ ;  $\hat{Z}' := \hat{Z}$  { Reject }
end if
Output  $\hat{Z}', (X'_{1:M}, T'_{1:M})$ 

```

Our Particle Gibbs Sampler, just as its classical counterpart, can include the additional step of parent sampling. However, we first describe the basic version (without parent sampling).

One step of PTGS (Poisson Tree Gibbs Sampler)

```

Input  $(X_{1:M}, T_{1:M})$  { Output of the previous step }
Run cPFPP to obtain  $(\mathcal{V}, \mathcal{E}, \mathbf{X}, \mathbf{T})$  { Tree with the distribution  $\psi_{\text{cond}}$  }
{ Select new  $S'$ : }
Select  $S' \in \mathcal{V}_{\text{end}}$  from the probability distribution  $\mathbb{P}(S' = s') \propto W_{s'}/C_{\text{pa}(s')}$ 
Output  $(X'_{1:M}, T'_{1:M}) := (X_{\text{an}(S')}, T_{\text{an}(S')})$ 

```

In fact, the main results are straightforward consequences of (3.3).

4.1 Proposition. *Let f be a nonnegative function on the space of skeletons $(x_{1:m}, t_{1:m})$ and $\pi(f) = \mathbb{E}_\pi f(X_{1:M}, T_{1:M})$. If the structure $(\mathcal{V}, \mathcal{E}, \mathbf{X}, \mathbf{T})$ is produced by PTPF then the following estimator of $z\pi(f)$ is unbiased:*

$$\widehat{z\pi(f)} = \begin{cases} \sum_{i \in \mathcal{V}_{\text{end}}} \frac{W_i}{C_{\text{pa}(i)}} f(X_{\text{an}(i)}, T_{\text{an}(i)}) & \text{if } \mathcal{V}_{\text{end}} \neq \emptyset; \\ 0 & \text{if } \mathcal{V}_{\text{end}} = \emptyset. \end{cases}$$

In particular, \hat{Z} is an unbiased estimator of z .

Proof. By (3.3), if $(\mathcal{V}, \mathcal{E}, \mathbf{X}, \mathbf{T}, S) \sim \phi$ then the marginal distribution of $(X_{\text{an}(S)}, T_{\text{an}(S)})$ is π . Therefore $\mathbb{E}_\phi f(X_{\text{an}(S)}, T_{\text{an}(S)}) = \pi(f)$. Again using (3.3), we see that

$$\psi(\mathcal{V}, \mathcal{E}, d\mathbf{x}, d\mathbf{t}) \frac{w_s}{c_{\text{pa}(s)}} = \hat{z}\psi(\mathcal{V}, \mathcal{E}, d\mathbf{x}, d\mathbf{t}, s) = z\phi(\mathcal{V}, \mathcal{E}, d\mathbf{x}, d\mathbf{t}, s),$$

where $(w_s/c_{\text{pa}(s)})/\hat{z} = \mathbb{P}_\psi(S = s|\mathcal{V}, \mathcal{E}, \mathbf{x}, \mathbf{t})$. Now it is enough to multiply both sides of the last display by $f(x_{\text{an}(s)}, t_{\text{an}(s)})$, integrate over $(d\mathbf{x}, d\mathbf{t})$ and sum over $s \in \mathcal{V}_{\text{end}}$ to obtain the result. Unbiasedness of \hat{Z} follows if we put $f \equiv 1$. \square

4.2 Theorem. *Markov chains generated by algorithms PTMH and PTGS have the equilibrium distribution equal to the target $\pi = \pi_{\text{post}}$ given by (2.4).*

Proof. The line of argument is almost the same as for the classical pMCMC algorithms with multinomial resampling. The crucial point is equation (3.3).

For PTMH, we use equation (3.3) to infer that

$$\frac{\hat{z}^*}{\hat{z}} = \frac{\phi(\mathcal{V}^*, \mathcal{E}^*, d\mathbf{x}^*, dt^*, s^*)\psi(\mathcal{V}, \mathcal{E}, d\mathbf{x}, dt, s)}{\phi(\mathcal{V}, \mathcal{E}, d\mathbf{x}, dt, s)\psi(\mathcal{V}^*, \mathcal{E}^*, d\mathbf{x}^*, dt^*, s^*)},$$

where $\hat{z}^*, \mathcal{V}^*, \mathcal{E}^*, \mathbf{x}^*, \mathbf{t}^*, s^*$ are new values produced by running PTMH, while $\hat{z}, \mathcal{V}, \mathcal{E}, \mathbf{x}, \mathbf{t}, s$ are values from the previous step. It follows that this algorithm is a proper Metropolis-Hastings procedure with the proposal distribution $\psi(\mathcal{V}, \mathcal{E}, d\mathbf{x}, dt, s)$ and the target $\phi(\mathcal{V}, \mathcal{E}, d\mathbf{x}, dt, s)$ on the space of configurations. The second equation in (3.3) shows that the distribution ϕ preserved by PTMH has the right marginal distribution $\pi(dx_{\text{an}(s)}, dt_{\text{an}(s)})$.

For PTGS, (3.3) shows that by running cPTPF we sample a configuration with the conditional distribution $\psi_{\text{cond}}(\mathcal{V}, \mathcal{E}, d\mathbf{x}, dt, s | x_{\text{an}(s)} = x_{1:m}, t_{\text{an}(s)} = t_{1:m})$. If, at the input, $(X_{1:m}, T_{1:m}) \sim \pi$ then configuration $(\mathcal{V}, \mathcal{E}, \mathbf{X}, \mathbf{T})$ obtained by PTPG has the distribution ϕ marginalised with respect to S . Consequently, after new S' has been chosen, we obtain $(\mathcal{V}, \mathcal{E}, \mathbf{X}, \mathbf{T}, S') \sim \phi$ with the marginal $(X_{\text{an}(S')}, T_{\text{an}(S')}) \sim \pi$ at the output. \square

4.3 REMARK. In this section we present particle methods (Particle Metropolis and Particle Gibbs) to sample hidden trajectory given static parameters based on Poisson resampling scheme. Now Bayesian inference on static parameters could be done by the same way as in standard PMCMC methods, for details we refer to [Andrieu et al. \(2010\)](#).

5 Variants and Extensions

In this section we present several variants and extensions of the basic algorithms. In particular we introduce the additional step of ancestor sampling in our particle Gibbs algorithm. The discussion is focused on two closely related issues. First is choosing the intensity parameters Λ_i . Second is parallelisation of computations.

In our description of algorithm PTPF, the step of choosing Λ_i s was left unspecified. We only assumed that $\Lambda_i = \mathbb{L}(\mathcal{H}(T_i))$, without any conditions on function \mathbb{L} . This assumption is sufficient to ensure that our algorithms are correct, i.e. the results in Section 4 and their proofs are valid. However, the efficiency of the algorithms crucially depends on the choice of Λ_i s. The intensity parameters control the size of the population of particles. It is equally undesirable to allow for an uncontrolled increase and for a rapid decrease (or even extinction) of the population.

One of our objectives is to construct algorithms in which computations are performed in a parallel way. In principle, perfectly parallel versions of PTPF, PTMH and PTGS are simple. If every parameter Λ_i depends only on $\text{an}(i)$, i.e. if we set $\mathbb{L}(\mathcal{H}(T_i)) = \mathbb{L}(X_{\text{an}(i)}, T_{\text{an}(i)})$ then the descendants of i evolve completely independently of other nodes not belonging to $\text{an}(i)$. However, this scenario is unrealistic, because it makes the number of particles impossible to control.

Another scenario is in some sense at the opposite extreme. Suppose that to control the number of particles, we allow Λ_i to depend on all the particles existing immediately before T_i , i.e. $\{j \in \mathcal{V} : T_{\text{pa}(j)} < T_i \leq T_j\}$. This makes parallel construction of algorithms much more difficult.

Discrete time models

We begin with the easier case of discrete time models. If time is discrete ($t = 1, \dots, m$) then $\mathcal{V}_t = \{i \in \mathcal{V} : T_i = t\}$ is t th “generation” of particles and all $i \in \mathcal{V}_t$ propagate simultaneously. It is natural to choose a

common value, $\Lambda_i = \Lambda_t$, for all $i \in \mathcal{V}_t$. An obvious way to stabilize the number of particles is to choose

$$(5.1) \quad \Lambda_t = \frac{\lambda_0}{\sum_{j \in \mathcal{V}_t} W_j},$$

because then $\mathbb{E}|\mathcal{V}_{t+1}| = \sum_{i \in \mathcal{V}_t} \Lambda_i W_i = \lambda_0$. Our simulations show that the rule (5.1) well stabilizes not only the expected number but also the actual number of particles, see the results presented in Section 6. Moreover, PTGS with the rule (5.1) is uniformly ergodic, under the same assumptions as for the standard Particle GS. Theorem 5.2 below and the method of proof are similar to (Lindsten et al., 2015). We verify a Doeblin condition for one step transition of discrete time PTGS. The proof of Theorem 5.2 is given in the Supplementary Material.

Recall that in a single step, PTGS takes a trajectory $X_{1:m}$ and outputs a new trajectory $X'_{1:m} = X_{\text{an}(S')}$. The target distribution $\pi = \pi_{\text{prior}}$ is given by (2.5). Symbol \mathbb{P} refers to the the transition probability of PTGS.

5.2 Theorem. *Consider discrete time PTGS with the rule (5.1). If the likelihood functions are uniformly bounded, i.e. $\|\ell_t\|_\infty = \sup_{x_t \in \mathcal{X}} \ell_t(x_t) \leq c < \infty$ then the following minorisation condition holds. For every measurable subset \mathcal{D} of \mathcal{X}^m and every $x_{1:m} \in \mathcal{X}^m$ we have*

$$\mathbb{P}(X'_{1:m} \in \mathcal{D} | X_{1:m} = x_{1:m}) \geq \varepsilon \pi(\mathcal{D}),$$

for some constant $\varepsilon > 0$.

This theoretical result confirms that under (5.1), PTGS is as efficient as its classical counterpart. Let us remark that Theorem 5.2 remains valid (with the same proof) also for PTGAS, the version of PTGS with ancestor sampling to be introduced in the next subsection.

Unfortunately, it is difficult to reconcile (5.1) with the parallel structure of computations. Some special properties of the Poisson distribution offer a possible way to overcome these difficulties and efficiently parallelise computations. Well-known techniques of “thinning” and “superposition” can be used in sampling the Poisson tree \mathbb{A} . We can use some preliminary approximation of $\sum_{j \in \mathcal{V}_t} W_j$ to compute “tentative” value of Λ_t at every time t . Then, in the next stage, the tree can be adjusted by sampling additional children and their descendants (superposition) or removing some children and their descendants (thinning). Another method is to use only a random sample of existing particles to determine Λ_t .

Ancestor sampling for discrete time models

Although algorithm PTGS does preserve π , its mixing properties are poor because of the well-known phenomenon of path-degeneration (as for the classical particle Gibbs Sampler). A remedy is to additionally resample parents, i.e. change those arrows in \mathcal{E} which lead to nodes in the (old) selected path. We adapt the method proposed in (Lindsten et al., 2014) to our Poisson tree setting.

For discrete time models, a modification of PTGS is straightforward and as simple as the original ancestor sampling in (Lindsten et al., 2014). The posterior is given by (2.5) and thus $W_i = \ell_t(X_i)$ for $i \in \mathcal{V}_t$. Assume that the intensity parameters are given by (5.1). In the following algorithm PTGAS-dt, we assume that the transition kernels $P_{t-1}(x_{t-1}, dx_t)$ are represented by transition *densities* $p_{t-1}(x_{t-1}, x_t)$.

Recall that according to notations used in cPTPF, $\text{an}(S) = (1, \dots, t, \dots, m)$. Therefore, in the pseudo-code below, instructions $j := t$; $i := t-1$ mean that we pick up an arrow belonging to the conditioning path (the input of cPTPF). Recall that $\mathcal{V}_t = \{i \in \mathcal{V} : T_i = t\}$.

One step of PTGAS-dt (Poisson Tree Gibbs with Ancestor Sampling - discrete time)

```

Input  $X_{1:m}$  { Output of the previous step }
Run cPFPF to obtain  $(\mathcal{V}, \mathcal{E}, \mathbf{X}, S)$  { Tree with the distribution  $\psi_{\text{cond}}$  }
 $\mathcal{E}'_0 := \mathcal{E}$ 
for  $t = 2, \dots, m$  do
    Let  $j := t$ ;  $i := t - 1$  {  $i \rightarrow j$  is an arrow in the conditioning path }
    Sample  $i' \in \mathcal{V}_{t-1}$  with probability  $\mathbb{P}(i') \propto W_{i'} p_{t-1}(X_{i'}, X_j)$ 
    { New parent of  $j$  }
     $\mathcal{E}'_t := (\mathcal{E}'_{t-1} \setminus \{i \rightarrow j\}) \cup \{i' \rightarrow j\}$  { Change arrow }
end for
 $\mathcal{E}' := \mathcal{E}'_m$ 
{ Select new  $S'$  }
Select  $S' \in \mathcal{V}_{\text{end}}$  from the probability distribution  $\mathbb{P}(S' = s') \propto W_{s'}$ 
Output  $X'_{1:m} := X_{\text{an}'(S')}$ 
{  $\text{an}'(\cdot)$  is the ancestor line corresponding to  $\mathcal{E}'$ , the new set of arrows }

```

5.3 Theorem. *Markov chain generated by algorithm PTGAS-dt has the equilibrium distribution equal to the target π .*

The proof is in the Supplementary Material.

Continuous time models

Choosing the intensity parameters is more difficult in the case of continuous time models. We have $W_i = \ell(X_i; T_{\text{pa}(i)}, T_i)$, thus W_i depends on the sample path Ξ_i in the time interval $[T_{\text{pa}(i)}, T_i]$. This means that the weights are actually assigned to arrows, not to nodes. It is not reasonable to compare likelihoods which correspond to different time intervals, so a formula analogous to (5.1) would make little sense. The solution we propose is in a sense a compromise between the two “extreme” scenarios sketched in the first part of this section. Roughly speaking, we partition the interval $[t_{\min}, t_{\max}]$ into subintervals or “strips”. The particles within every strip evolve independently. At the end of the strip we synchronise the particles and compute some statistic which is used to determine Λ_i s in the next strip.

We proceed to details. The points of partition (arbitrarily chosen) are

$$t_{\min} = t_{\text{syn}}^0 < t_{\text{syn}}^1 < \dots < t_{\text{syn}}^r < \dots < t_{\text{syn}}^q = t_{\max}$$

(t_{syn} standing for ‘synchronisation time’). Let

$$\mathcal{F}^r = \{i : t_{\text{syn}}^r \leq T_i < t_{\text{syn}}^{r+1}\}.$$

If $i \in \mathcal{F}^r$ then we say that particle i is in r th strip, i.e. has a chance to propagate in the interval $[t_{\text{syn}}^r, t_{\text{syn}}^{r+1}]$. Let

$$\mathcal{F}_\circ^r = \{i : T_{\text{pa}(i)} < t_{\text{syn}}^r \leq T_i < t_{\text{syn}}^{r+1}\} \text{ and } \mathcal{G}^r = \{i : T_{\text{pa}(i)} < t_{\text{syn}}^r, T_i \geq t_{\text{syn}}^{r+1}\}.$$

Note that $\mathcal{F}^r \setminus \mathcal{F}_\circ^r$ is the set of nodes in \mathcal{F}^r whose parents are also in \mathcal{F}^r . The number of particles that exist immediately before time t_{syn}^r is $|\mathcal{F}_\circ^r \cup \mathcal{G}^r|$. For every $i \in \mathcal{F}_\circ^r$, let

$$W_i^r = \ell(\Xi_{i[t_{\text{syn}}^{r-1}, t_{\text{syn}}^r]})$$

be the partial likelihood corresponding to the path Ξ_i in the *previous* strip (whilst $W_i = \ell(\Xi_{i[t_{\text{pa}(i)}, t_i]})$). Let

$$W_\circ^r = \sum_{i \in \mathcal{F}_\circ^r} W_i^r.$$

Let us emphasise that the likelihoods for different paths are computed for the same time interval $[t_{\text{syn}}^{r-1}, t_{\text{syn}}^r[$. Now, we propose the following rule of computing Λ_i s in r th strip. Choose a nondecreasing function $b :] - \infty, \infty[\rightarrow [0, \infty]$. Assume that $\mathcal{F}_\circ^r \neq \emptyset$ and put

$$(5.4) \quad \Lambda_i = \begin{cases} \frac{1}{W_i} \frac{W_i^r}{W_\circ^r} b(\lambda_0 - |\mathcal{G}^r|) & \text{for } i \in \mathcal{F}_\circ^r; \\ \frac{1}{W_i} & \text{for } i \in \mathcal{F}^r \setminus \mathcal{F}_\circ^r. \end{cases}$$

The idea behind this seemingly complicated formula is simple. To begin with, λ_0 is the expected *initial* number of particles. We would like to keep the number of particles as close to λ_0 as possible, in the course of building the tree. To this end, we try to control the Poisson intensities $\Lambda_i W_i$. Note that under (5.4) we obtain

$$\sum_{i \in \mathcal{F}_\circ^r} \Lambda_i W_i = b(\lambda_0 - |\mathcal{G}^r|).$$

This expression is the expected number of children of nodes in \mathcal{F}_\circ^r (conditioned on the history of the process before t_{syn}^r). The second line in (5.4) implies that for every node in $\mathcal{F}^r \setminus \mathcal{F}_\circ^r$, the expected number of children is one. Particles corresponding to \mathcal{G}^r “pass through” the strip $[t_{\text{syn}}^r, t_{\text{syn}}^{r+1}[$ unchanged. Putting this together, we see that the (conditional) expected number of particles that exist immediately before t_{syn}^{r+1} is

$$b(\lambda_0 - |\mathcal{G}^r|) + |\mathcal{G}^r|.$$

If we put $b(l) = \max(l, 0)$ then the expected number of particles immediately before t_{syn}^{r+1} would be equal to $\max(\lambda_0, |\mathcal{G}^r|)$. However, if $|\mathcal{G}^r| \geq \lambda_0$ then the particles in \mathcal{F}^r would have zero chance to propagate. Therefore, a reasonable strategy is to choose e.g. $b(l) = \max(l, b_0)$ for some small constant $b_0 > 0$.

Equation (5.4) involves, apart from the quantities specific to node i , only sets \mathcal{F}_\circ^r , \mathcal{G}^r and the sum of weights W_\circ^r . This means that we have to identify all the particles which exist at moment t_{syn}^r , know their lifespans and locations before we proceed to processing nodes in \mathcal{F}^r . On the other hand, *we need not sort T_i s for $i \in \mathcal{F}_\circ^r$* . This fact is important for efficient implementation of the algorithm. Once we create children of nodes in \mathcal{F}_\circ^r , we compute their lifespans and identify nodes in $\mathcal{F}^r \setminus \mathcal{F}_\circ^r$. Descendants of every node in \mathcal{F}_\circ^r evolve independently until t_{syn}^{r+1} , the next moment of synchronisation.

Ancestor sampling for continuous time models

For continuous time models, ancestor sampling is more complicated. The general idea is the same as in (Lindsten et al., 2014). In PTGS, we change the parents of nodes along the input path in such a way that preserves ϕ , the extended target distribution. However, the details are more difficult, due to the complicated rules for computing Λ_i s. Assume that the intensity parameters are given by (5.4). Our procedure of ancestor sampling is based on the following idea. We change an existing arrow $i \rightarrow j$ to a new arrow $i' \rightarrow j$ only if $j \in \mathcal{F}^r \cap \mathcal{G}^{r-1} \cap \text{an}(S)$ and furthermore if i and i' belong to the same “synchronisation strip” (say \mathcal{F}^p with $p < r - 1$). Under these conditions we are able to compute the ratio between ϕ distributions for the old configuration and the new one. In the pseudo-code below we write $W_{i' \rightarrow j} = \ell(X_j; T_{i'}, T_j)$. Assume also that the transition kernel $K(x_{k-1}, t_{k-1}, dx_k, dt_k)$ is represented by transition density $k(x_{k-1}, t_{k-1}, x_k, t_k)$.

One step of PTGAS-ct (Poisson Tree Gibbs with Ancestor Sampling - continuous time)

Input $(X_{1:M}, T_{1:M})$ { **Output of the previous step** }
 Run cPFPF to obtain $(\mathcal{V}, \mathcal{E}, \mathbf{X}, \mathbf{T}, S = M)$ { **A tree with the conditional distribution ψ_{cond}** }

```

 $\mathcal{E}'_0 := \mathcal{E}$ 
for  $t = 2, \dots, M$  do
  Let  $j := t$ ;  $i := t - 1$  {  $i \rightarrow j$  is  $t$ th arrow along the conditioning path }
  Find  $r$  such that  $j \in \mathcal{F}^r$ 
  { If  $j \notin \mathcal{G}^{r-1}$  then do nothing }
  if  $j \in \mathcal{G}^{r-1}$  then
    Find  $p$  such that  $i \in \mathcal{F}^p$ 
    Sample  $i' \in \mathcal{F}^p$  with probability
      
$$\mathbb{P}(i') \propto \frac{W_{i'} W_{i' \rightarrow j} \cdot k(X_{i'}, T_{i'}; X_j, T_j)}{C_{\text{pa}(i')}}$$

     $\mathcal{E}'_t := (\mathcal{E}'_{t-1} \setminus \{i \rightarrow j\}) \cup \{i' \rightarrow j\}$ 
    { Sample a new parent of  $j$  and change arrows }
  end if
   $\mathcal{E}' := \mathcal{E}'_M$ 
end for
for all  $i \in \mathcal{V}_{\text{end}}$  do
  Recompute  $C_{\text{pa}'(i)} = \prod_{j \in \text{an}'(i) \setminus \{i\}} \Lambda_j$ 
  { an'( $\cdot$ ) and pa'( $\cdot$ ) correspond to  $\mathcal{E}'$ , the new set of arrows }
end for
{ Select new  $S'$ : }
Select  $S' \in \mathcal{V}_{\text{end}}$  from the probability distribution  $\mathbb{P}(S' = s') \propto W_{s'} / C_{\text{pa}'(s')}$ 
Output  $(X'_{1:M'}, T'_{1:M'}) := (X_{\text{an}'(S')}, T_{\text{an}'(S')})$ 

```

The following theorem shows that the ancestor sampling step is correct.

5.5 Theorem. *Markov chain generated by algorithm PTGAS-ct has the equilibrium distribution equal to the target π .*

The proof is based on the following observations:

- For any q sets of nodes \mathcal{F}^q , \mathcal{G}^q and \mathcal{F}_o^q remain unchanged if $i \rightarrow j$ is replaced by $i' \rightarrow j$ (because i and i' belong to the same strip).
- Since $j \in \mathcal{G}^{r-1}$ we ensure that $W_j^r = \ell(\Xi_{j[t_{\text{syn}}^{r-1}, t_{\text{syn}}^r]})$ remains unchanged. Indeed, the assumptions in Section 2 imply that $\Xi_{j[t, T_j]}$ is uniquely determined by X_j and does not depend on $\text{pa}(j)$, provided that $T_{\text{pa}(j)} < t$ (see (2.1) and comments following this equation).

The full proof of Theorem 5.5 is relegated to the Supplementary Material.

6 Simulation results

In this section we examine PTPF's properties in a series of numerical evaluations. To assess the overall correctness of PTPF scheme in discrete time setting we compare our implementation with PGAS from (Lindsten et al., 2014). In subsequent sections we investigate properties of continuous time PTPF and implementation details.

Discrete time models

Here we study differences between PTPG and classical Gibbs sampler in the setting of discrete time processes. To this end we examine two state space models – stochastic volatility model and simple non-linear model considered in (Andrieu et al., 2010). Both algorithms have been run on the same sets of starting and observed trajectories.

A non-linear state space model

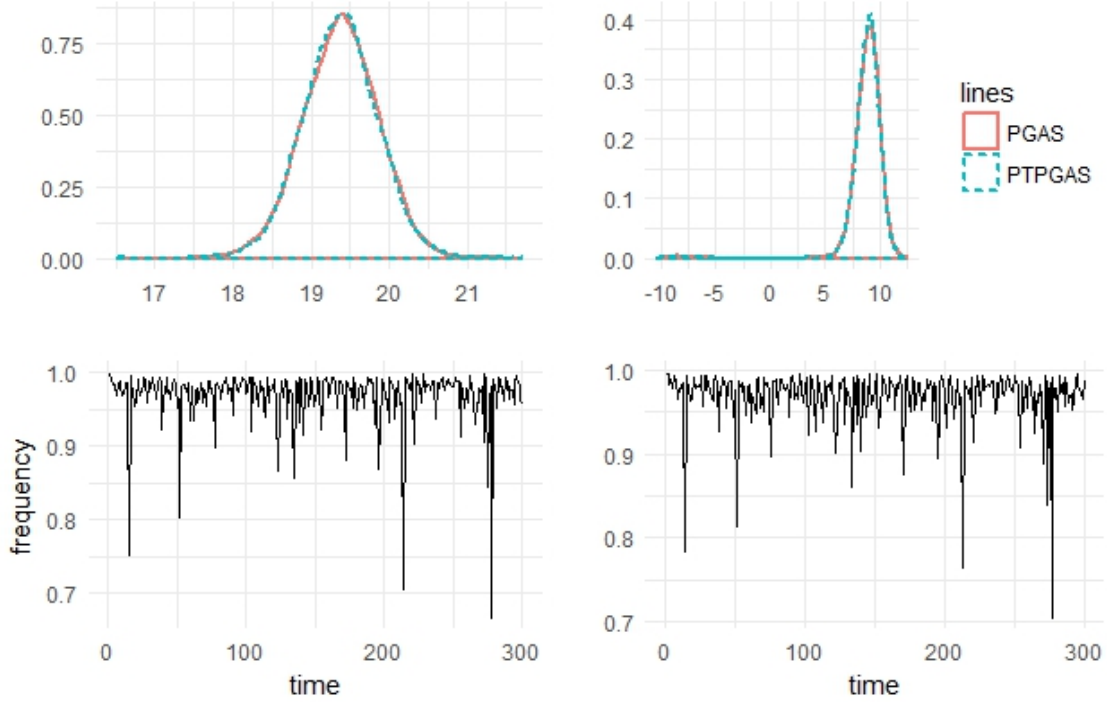


Figure 1: Estimated densities of 100'th (upper left corner) and 200'th state (upper right corner). Bottom row - comparison of update frequency for last 1000 iterations between PGAS (left) and PTPGAS (right)

We start our study with a simple non-linear state space model given by equations:

$$X_k = \frac{X_{k-1}}{2} + 25 \frac{X_{k-1}}{1 + X_{k-1}^2} + 8 \cos(1.2k) + V_k$$

$$Y_k = \frac{X_k^2}{20} + W_k,$$

where $X_1 \sim \mathcal{N}(0, 5)$, $V_n \sim \mathcal{N}(0, \sigma_V^2)$, $W_n \sim \mathcal{N}(0, \sigma_W^2)$.

Priors for both parameters have been set to $\mathcal{IG}(0.01, 0.01)$ with $(N, \lambda_0, T) = (300, 300, 300)$. Both algorithms have been run for 10 000 iterations with 3000 burnin and starting parameters equal to: $\sigma_V^2 = 10$, $\sigma_W^2 = 1$.

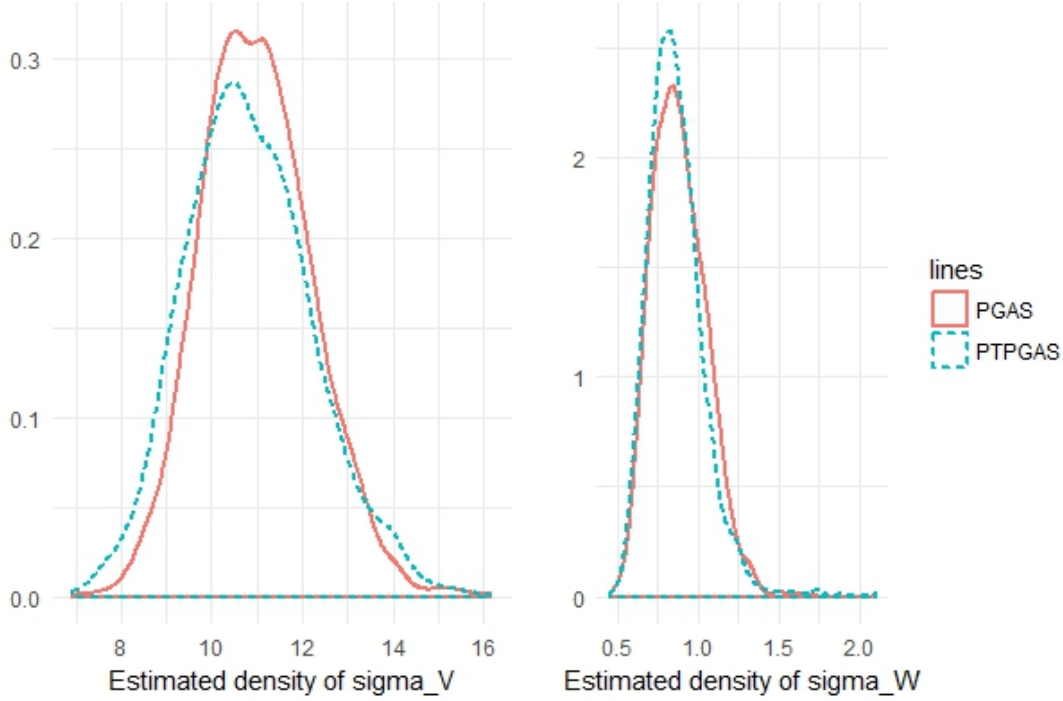


Figure 2: Estimated densities of models' parameters in non-linear state space model

Stochastic Volatility Model with Leverage

Next we consider the model governed by equations:

$$\begin{aligned} X_{k+1} &= \mu(1 - \phi) + \phi \cdot X_k + \sigma \cdot \mathcal{N}(0, 1) \\ Y_k &= e^{(-0.5X_k)} \cdot \mathcal{N}(0, 1) \end{aligned}$$

Priors and sampling method were taken from (Kim et al., 1998). Observations have been taken from Standard and Poors (SP) 500 data for the interval 2017-03-10 – 2018-05-17.

Both algorithms have been run for 10 000 iterations with 5000 burnin and $(N, \lambda_0) = (1000, 1000)$. Trajectory length has been set to 300.

For both the models we have not found any significant differences between classical particle Gibbs Sampler and the Poisson Tree scheme. Posterior estimates obtained with PTPG may manifest higher share of outliers – a phenomenon which exhibits itself in estimate of σ in figure 4 – nonetheless the speed and quality of convergence seems to be comparable. Both ancestor sampling schemes seem to provide equivalent improvement in mixing. The obvious disadvantage of PTPG is a little bit more involved implementation.

Continuous time models

Here we apply PTPG to two PDSMPs which have been considered among others in (Finke et al., 2014) to illustrate its properties and assess the overall utility of ancestor sampling step.

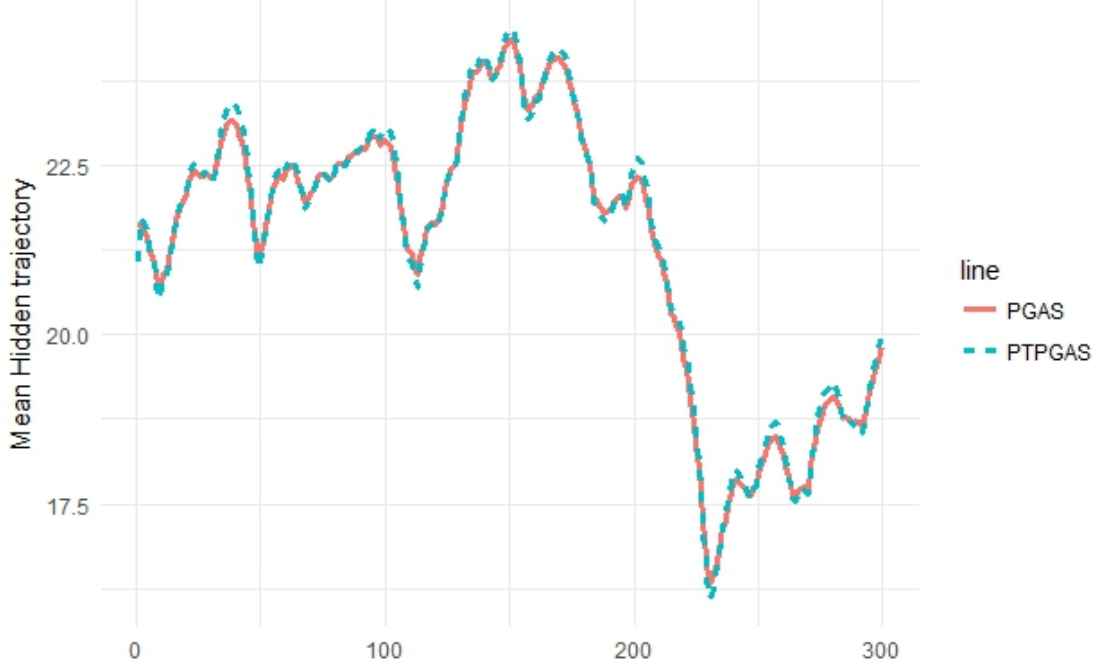


Figure 3: Comparison of mean sampled trajectory after burnin of 5000 for stochastic volatility model

In both the examples b function (which controls the size of population) has been defined by

$$b(x) = \begin{cases} x, & x \geq 1; \\ 0.9x + 0.1, & 0 \leq x < 1; \\ 0.1, & x < 0. \end{cases}$$

Elementary change-point model

For a first example we have used a simple PDP in which skeleton of Ξ is assumed to be $AR(1)$ process (with coefficient ρ) with unknown variance of noise, σ . Jump times are sampled from gamma distribution with unknown parameters α, β and mean $\alpha \cdot \beta$. Observations are assumed to be taken at ends of fixed time intervals (in our example $[n, n + 1[$ for $n \in \mathbb{N}$) and formed by adding mean 0 Gaussian noise with variance σ_y to Ξ .

Data used for simulations have been sampled with static parameters equal to $(\alpha, \beta, \rho, \sigma, \sigma_y) = (2, 2, 0.9, 1, 2)$. α and β were both given uniform priors on $[0, 10]$ whilst the remaining parameters $(\rho, \sigma, \sigma_y) \sim \mathcal{N}(0, 10)$ truncated to \mathbb{R}_+ . Synchronization strips were taken to be $[n, n + 1[$ for $n \in \mathbb{N}$.

Figure 5 shows comparison of the mean sampled trajectory with the real hidden trajectory for the last 30 000 iterations of run of 80 000 iterations (with $\lambda_0 = 3000$). For additional reference every 200th sampled trajectory has been plotted (red colour). Posterior distribution of gamma parameters has been sampled with 15000 iterations of independent Metropolis - Hastings algorithm with $Unif(0, 10)$ kernel. Remaining posteriors have been approximated with 15000 runs of Gaussian random walk Metropolis - Hastings (one run for pair (ρ, σ) and one for σ_y) with variance of kernel set to 1. Estimated posterior densities can be seen in Figure 6.

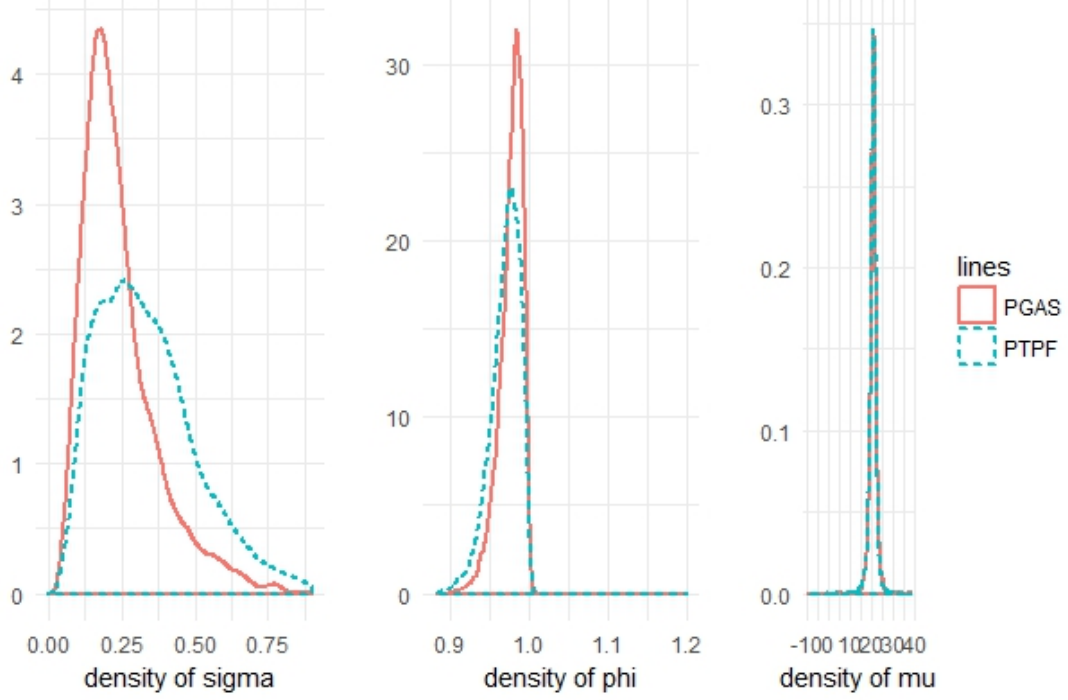


Figure 4: Comparison of estimated parameters' densities for stochastic volatility model with leverage

Shot-noise-Cox-process model

The model assumes observations Υ to be an inhomogenous Poisson process with intensity modeled by latent intensity $(\xi(t), t \in [0, T])$ sampled from Ξ .

Ξ is assumed to be a piecewise deterministic process, governed by kernel with density:

$$k(x_{n-1}, t_{n-1}; x_n, t_n) = \lambda_t \cdot e^{-\lambda_t \cdot (t_n - t_{n-1})} \cdot \mathbb{1}_{(t_n - t_{n-1} > 0)} \cdot \lambda_\phi \cdot e^{-\lambda_\phi \cdot (x_n - \bar{x}_{n-1})} \cdot \mathbb{1}_{(x_n - \bar{x}_{n-1} > 0)}$$

where $\bar{x}_m = x_m \cdot e^{-\kappa \cdot (t_m - t_{m-1})}$

For our simulations we have chosen

$$\kappa = 0.01, \lambda_t = \frac{1}{40}, \lambda_\phi = \frac{2}{3}, T = 1000$$

with synchronisation at integer time-points and priors (truncated to \mathbb{R}_+)

$$(\kappa, \lambda_t, \lambda_\phi) \sim \mathcal{N}(0, 1) \times \mathcal{N}(0, 10) \times \mathcal{N}(0, 10).$$

Sampling from the posterior distribution has been approximated by 2 runs of Gaussian random-walk Metropolis-Hastings algorithm (2000 iterations each) targeting:

$$\lambda_t \sim \pi(\lambda_t | \xi, \Upsilon) \quad (\kappa, \lambda_\phi) \sim \pi(\kappa, \lambda_\phi | \xi, \Upsilon).$$

(where ξ is a trajectory sampled in antecedent run of PTPG)

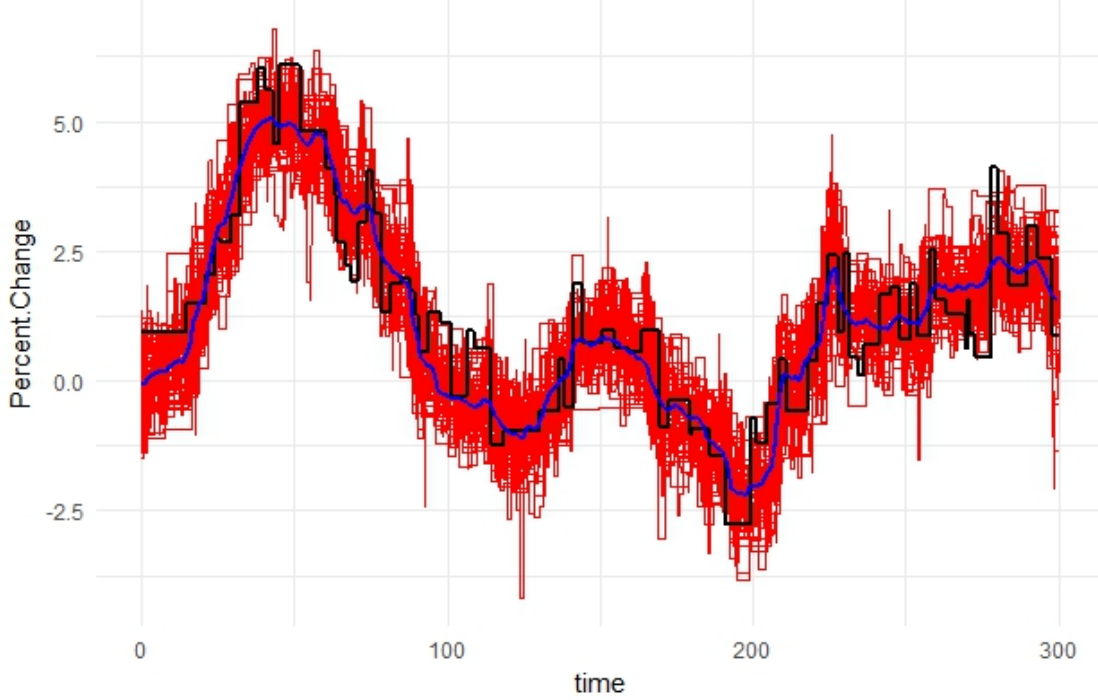


Figure 5: Mean sampled trajectory (blue) vs true hidden trajectory (black) for elementary change point model

Figures 7, 8 show the result of 80 000 iterations of PTGAS with 50 000 burning and $\lambda_0 = 1000$.

Figure 10 depicts update frequency (calculated every 0.5 time-step) for Poisson Tree Gibbs sampler with (left) and without ancestor sampling (right). It is evident that the ancestor sampling step enhances mixing, though the results still look worse than in the discrete time setting. Adjustment of synchronisation strips size to jumps' distribution is of crucial importance for ancestor sampling performance. At least one pilot run is needed to better adjust parameters to data.

We have found that without ancestor sampling the algorithm tends to get stuck at short trajectories (in the sense of number of jumps) for a few iterations. This phenomenon is presumably caused by the fact that short trajectories have potentially smaller accumulated ancestors' weights and thus their final weights (i.e. weights used to choose a new fixed trajectory) have an order of magnitude bigger than that of longer trajectories. This may probably be additionally countered by introduction of virtual jumps or adaptive size of synchronisation strips but we have not pursued those approaches any further.

Figure 9 shows data on the number of surviving particles for first 1000 iterations of Shot-noise-Cox-process model. Top row displays histogram and time series of population size for 700 time step. 95% of iterations stay within range of 17 from desirable magnitude. Bottom row depicts mean and standard deviation of number of surviving particles at the end of every synchronisation strip. It is clear that the employed strategy is effective at controlling size of population – after a mild burst at the end of first synchronisation strip number of particles stabilizes barely overshooting [990, 1010] interval.

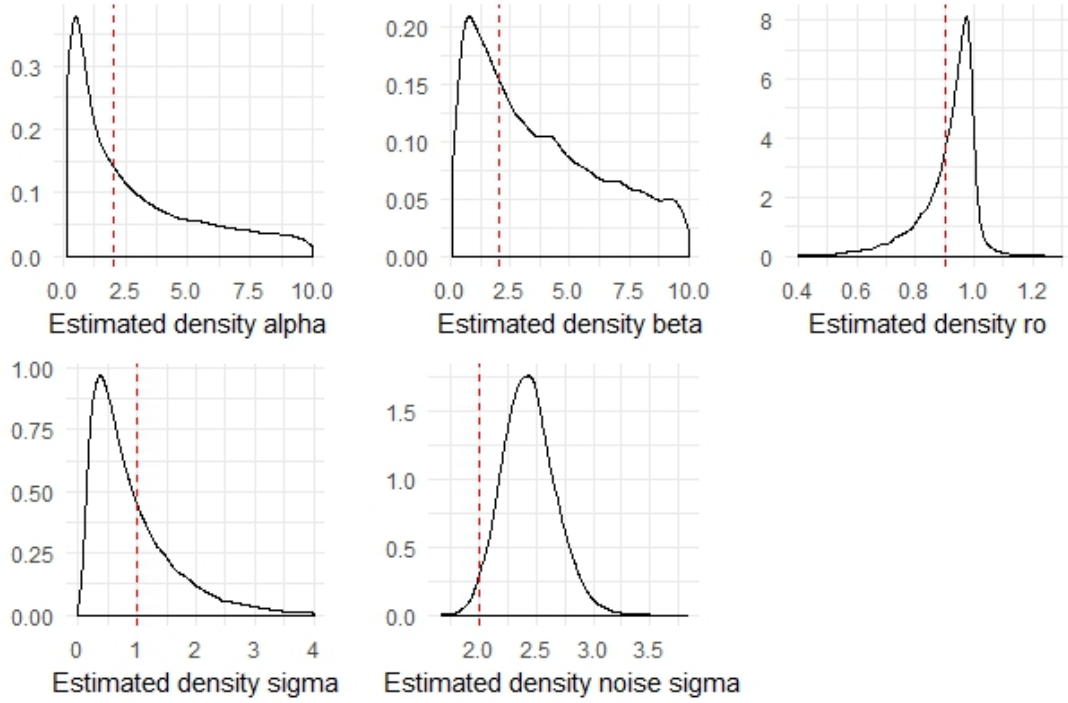


Figure 6: Estimated densities of static parameters in elementary change point model

Implementation and performance comparison

A non-linear state space model from section 6 has been used for comparison between classical Particle Gibbs sampler and Poisson Tree scheme. The two algorithms have been implemented in C++ and employed utilities from standard library. Time measurements have been obtained from runs on 64 cores, 2.5GHz per each. For both approaches computations were performed by fixed number of threads working in parallel (plus one additional thread in case of PTPF whose sole purpose of existence was to gather sums of weights from each thread, combine them and redistribute result amongst workers).

Distribution of work between finite number of worker threads is straightforward in the setting of classical Particle Filter but gets more troublesome with introduction of PTPF – one can still divide first population uniformly between threads letting each thread take care of its own batch but we have found that after average batch to thread ratio decreases beyond a certain point (we have empirically observed this threshold to be around 500 particles per thread) some batches perish completely after few dozens of propagations. To counter this erratic behaviour every 50 steps we synchronize all threads and let one chosen thread redistribute surviving particles uniformly. Despite the additional overhead introduced by this operation we have found this modified scheme to be more effective. The detailed comparison of our parallel implementation with approaches presented in (Paige et al., 2014a; Murray et al., 2016) is discussed in Supplementary Material.

Figure 11 shows the comparison of mean times of execution (in milliseconds) for 10 iterations, trajectory length equal to 400 and number of threads working in parallel equal to 50. For big population to thread ratio PTPG provides much faster time of execution. However, we have found that its time of execution exhibits larger variance between different runs. Both algorithms scale quite well with increasing number of threads but ordinary Particle Gibbs sampler seems to be more resistant to decrease in number of threads – for instance after reduction to only 10 worker threads execution time for one million is around 50s for PG and 20s for PTPG. When number of particles is smaller than 3000 parallel PTPF implementation ceases to

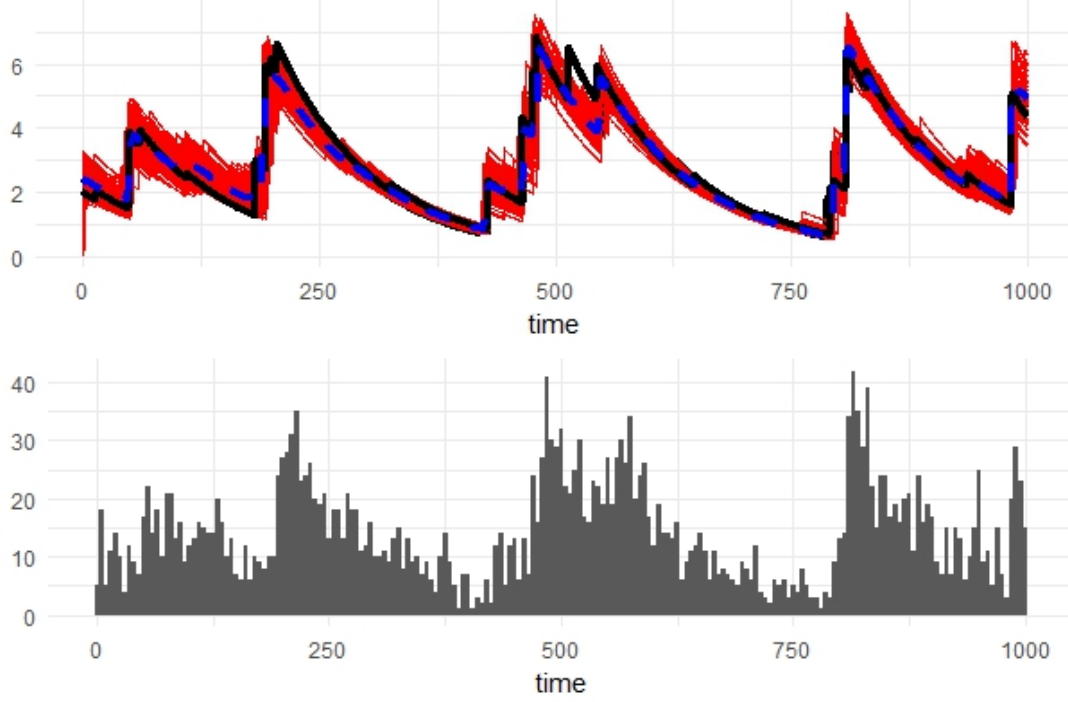


Figure 7: Mean (blue) sampled trajectory vs hidden trajectory for Shot-noise-Cox-process model

be practicable.

Implementation of the algorithm for continuous time is considerably more involved, hence an efficient implementation encompassing both schemes is not feasible. Apart from death time and weight one has to keep information about accumulated parent weight, weight truncated to synchronisation strip, time of birth and strip of death. Additional bookkeeping is necessary – for every synchronisation strip $|\mathcal{G}^r|, b(\lambda_0 - |\mathcal{G}^r|)$ must be recorded. Particles which have not propagated are kept on stacks – one for every synchronisation strip. Particles after propagation are stored in vectors (analogously one for every synchronisation strip). This enforces much greater movement of data from one place to another (which is essentially constant in discrete time setting).

Acknowledgement

The paper is partially supported by Polish National Science Center grant: NCN UMO-2018/31/B/ST1/00253.

A Semi-Markov Piece-wise Deterministic Processes

Here we provide a more detailed and explicit description of a class of processes we consider. Let \mathcal{X} be a Polish space (a complete and separable metric space equipped with its Borel σ -field). A *piece-wise deterministic semi-Markov process* (PDSMP) $\Xi = \{\Xi(t), t \geq t_{\min}\}$ is a process with values in \mathcal{X} which evolves deterministically in continuous time except for a countable collection of stopping times at which it randomly jumps. Trajectories of Ξ are càdlàg (right continuous functions having left limits). Jumps are described

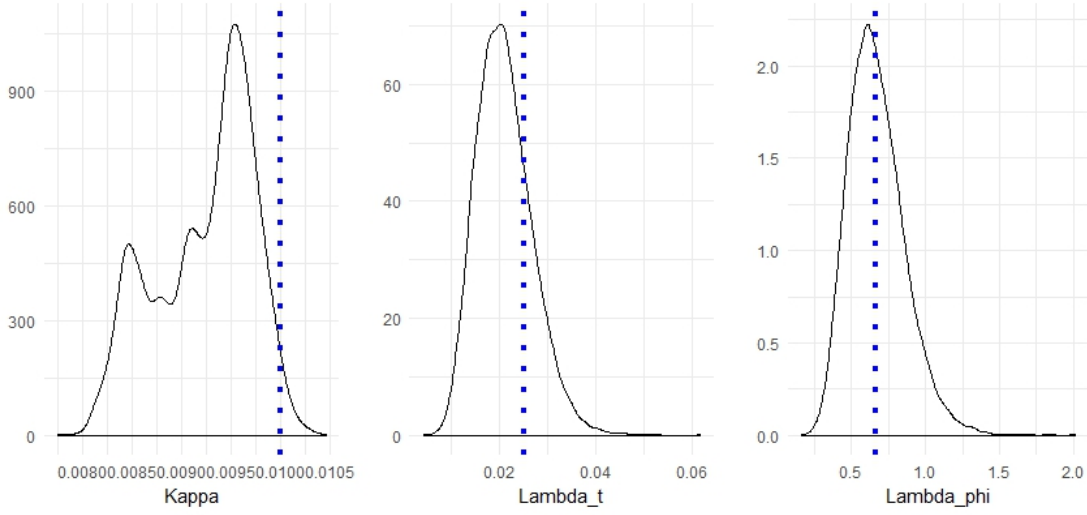


Figure 8: Estimated densities of static parameters for Shot-noise-Cox-process model

by a space-time stochastic transition kernel $\tilde{K} = \tilde{K}(x_{k-1}, t_{k-1}; d\tilde{x}_{k-1}, dt_k)$ and by an initial distribution $\tilde{\nu} = \tilde{\nu}(d\tilde{x}_0, dt_1)$. Deterministic dynamics between jumps is described by a function $G : \mathcal{X} \times [t_{\min}, \infty[^2 \rightarrow \mathcal{X}$ which satisfies $G(x, t, t) = x$ and $G(x, t, t'') = G(G(x, t, t'), t', t'')$ for $t \leq t' \leq t''$. We additionally require that the function $t' \mapsto G(x, t, t')$ is continuous for all $x \in \mathcal{X}$, $t \in [t_{\min}, \infty[$ and the map $x \mapsto G(x, t, t')$ is one-to-one for any $t \leq t'$.

Evolution of the process is described in the following steps. The times of jumps are denoted by $T_1 < \dots < T_k < \dots$. By convention, $T_0 = t_{\min}$. Let $X_k = \Xi(T_k-)$ and $\tilde{X}_k = \Xi(T_k)$. We define the rules of transitions $(X_{k-1}, T_{k-1}) \rightarrow (\tilde{X}_{k-1}, T_k) \rightarrow (X_k, T_k)$, where the first move is governed by \tilde{K} and the second by G :

$$(A.1) \quad \begin{aligned} \mathbb{P}(\tilde{X}_{k-1} \in d\tilde{x}_{k-1}, T_k \in dt_k | X_{k-1} = x_{k-1}, T_{k-1} = t_{k-1}) &= \tilde{K}(x_{k-1}, t_{k-1}; d\tilde{x}_{k-1}, dt_k), \\ X_k &= G(\tilde{X}_{k-1}, T_{k-1}, T_k). \end{aligned}$$

Then we put

$$(A.2) \quad \Xi(t) = G(\tilde{X}_{k-1}, T_{k-1}, t), \text{ for } T_{k-1} \leq t < T_k.$$

To simplify notation, let us introduce a fictitious state x_0 and put $t_0 = t_{\min}$. By convention we can write the initial distribution as $\tilde{\nu}(d\tilde{x}_0, dt_1) = \tilde{K}(x_0, t_0; d\tilde{x}_0, dt_1)$. Consequently, equation (A.1) makes sense also for $k = 1$ and (A.2) completely describes $\Xi = \{\Xi(t), t \geq t_{\min}\}$.

In order to facilitate description of our algorithm PTPF and the construction of our ancestor sampling, we have chosen to work with the skeleton

$$(A.3) \quad (X_1, T_1), \dots, (X_k, T_k), \dots$$

Note that, according to the definitions above, X_k is the value *at the end* of k th deterministic piece of a trajectory. The sequence (A.3) is a Markov chain with the transition kernel $K = K(x_{k-1}, t_{k-1}; dx_k, dt_k)$ implicitly defined via the two transitions in (A.2). Under the convention introduced earlier, the initial distribution can be expressed as $\mathbb{P}(X_1 \in dx_1, T_1 \in dt_1) = K(x_0, t_0; dx_1, dt_1)$. To ensure that (A.3) uniquely defines Ξ , we have assumed that the map $x \mapsto G(x, t, t')$ is one-to-one for any $t \leq t'$. Consequently, \tilde{X}_{k-1} is a function of (X_k, T_{k-1}, T_k) . Let us note that in order to recover the trajectory $(\Xi(t), T_{k-1} \leq t < T_k)$, we have to follow the deterministic dynamics in the reverse direction, starting from $X_k = \Xi(T_k-)$ and proceeding

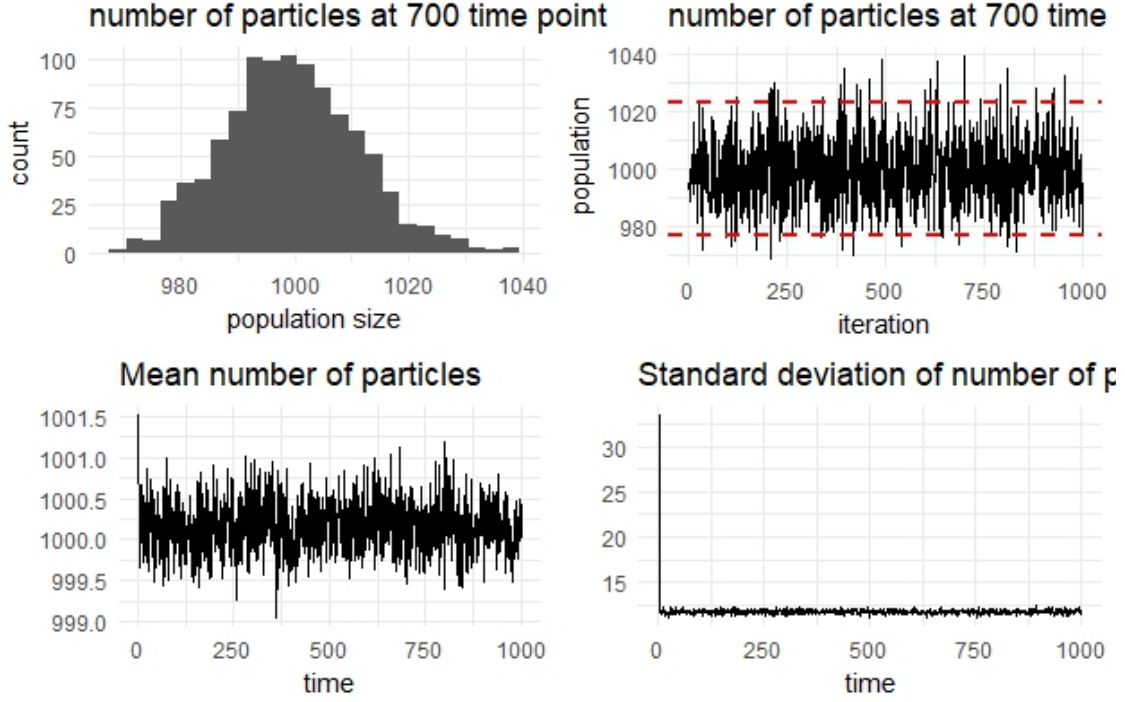


Figure 9: Number of particles for 100 iterations

backwards. This is perhaps not easy in general but feasible in many concrete models. For the important class of piece-wise constant processes it is trivial.

A wide subclass of PDSMPs consists of continuous time *piece-wise deterministic Markov processes* (PDMPs). Assume that we have a nonnegative function Q on $\mathcal{X} \times [t_{\min}, \infty[$, interpreted as the intensity of jumps and a family of kernels $P_t = P_t(x, d\tilde{x})$ which govern state transitions. The transition rules (A.2) now reduce to

$$\begin{aligned} \mathbb{P}(\tilde{X}_{k-1} \in d\tilde{x}_{k-1} | X_{k-1} = x_{k-1}, T_{k-1} = t_{k-1}) &= P_{t_{k-1}}(x_{k-1}, d\tilde{x}_{k-1}), \\ \mathbb{P}(T_k > t | \tilde{X}_{k-1} = \tilde{x}_{k-1}, T_{k-1} = t_{k-1}) &= \exp \left[- \int_{t_{k-1}}^t Q(G(\tilde{x}_{k-1}, t_{k-1}, u), u) du \right], \\ X_k &= G(\tilde{X}_{k-1}, T_{k-1}, T_k). \end{aligned}$$

It is easily seen that the continuous time process Ξ given by (A.2) is Markov (in general, inhomogeneous in time). A rigorous proof can be found in (Davis, 1984). Homogeneous PDMPs obtain if the intensity function does not depend on time, i.e. $Q(x, t) = Q(x)$, the kernels P_t do not depend on t and $G(x, t, t')$ depends on (t, t') only through $t' - t$. In particular, our setup covers *piece-wise constant homogeneous* Markov processes. In this important special case we have $G(x, t, t') = x$, $\tilde{X}_{k-1} = X_k$ and

$$\begin{aligned} \mathbb{P}(X_k \in dx_k | X_{k-1} = x_{k-1}, T_{k-1} = t_{k-1}) &= P(x_{k-1}, dx_k), \\ \mathbb{P}(T_k > t | X_k = x_k, T_{k-1} = t_{k-1}) &= \exp [-(t - t_{k-1})Q(x_k)]. \end{aligned}$$

Now we proceed to models in which process Ξ is hidden and we observe a random element Y which depends on Ξ . The likelihood is the probability of observing $\Upsilon = y$, given sample path ξ of Ξ . Since y is fixed and need not be explicitly indicated, it will be dropped from notation whenever no misunderstanding can occur.

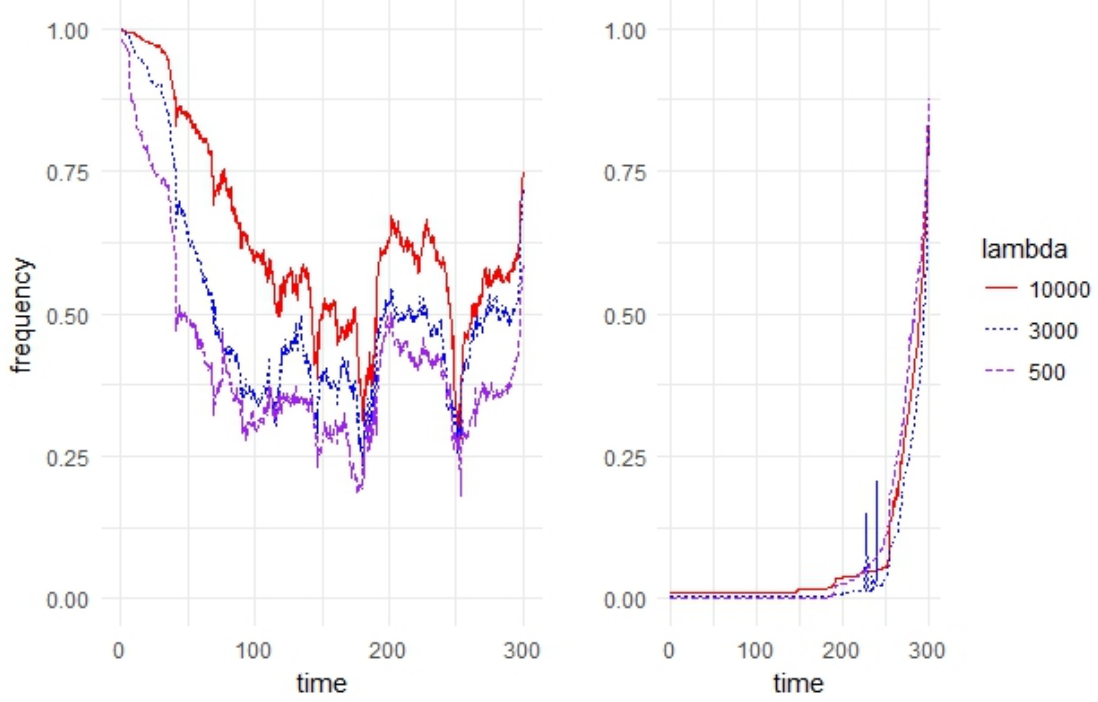


Figure 10: Update frequency for 1000 iterations of elementary change point model

We are going to describe typical forms of likelihood functions $\ell(\xi_{[t,t']})$, where $\xi_{[t,t']} = \{\xi(t), t \leq t < t'\}$. We always require that these functions satisfy the condition (2.3): or $t < t' < t''$,

$$\ell(\xi_{[t,t'']}) = \ell(\xi_{[t,t']})\ell(\xi_{[t',t'']}).$$

In many applications, the observation process Υ is just a sequence of “noisy measurements” of the process Ξ at discrete “observation times”, say $t_{\min} \leq t_{\text{obs}}^1 < \dots < t_{\text{obs}}^p \leq t_{\max}$. Formally, we assume that $\Upsilon = (Y_1, \dots, Y_p)$, where each Y_r is sampled independently from a (possibly time-dependent) probability density $\ell_r(\cdot | \xi(t_{\text{obs}}^r))$. The likelihood functions in this model are given by

$$(A.4) \quad \ell(\xi_{[t,t']}) = \prod_{t \leq t_{\text{obs}}^r < t'} \ell_r(y_r | \xi(t_{\text{obs}}^r))$$

and clearly fulfil the assumption (2.3). A standard example would be adding a Gaussian noise to observations on a hidden continuous time Markov process, see for example simple prey-predator model considered in (Golightly and Wilkinson, 2011).

Another form of likelihood may be obtained if Υ is a continuous time Markov process. Assume that the state space \mathcal{Y} of this process is finite and the transition intensities of Υ depend on a current state of Ξ . Let $Q_{\Upsilon}(v, v' | x)$ be the intensity of transitions from $v \in \mathcal{Y}$ to $v' \in \mathcal{Y}$, $v' \neq v$, if $\Xi(t) = x$. The intensity of jumps out of v is $Q_{\Upsilon}(v | x) = \sum_{v' \neq v} Q_{\Upsilon}(v, v' | x)$. For definiteness, assume that trajectories of Υ are right continuous. If we observe $\Upsilon = y$ then the likelihood is given by

$$(A.5) \quad \ell(\xi_{[t,t']}) = \prod_{\substack{u: y(u-) \neq y(u) \\ t \leq u \leq t'}} Q_{\Upsilon}(y(u-), y(u) | \xi(u)) \exp \left[- \int_t^{t'} Q_{\Upsilon}(y(u) | \xi(u)) du \right]$$

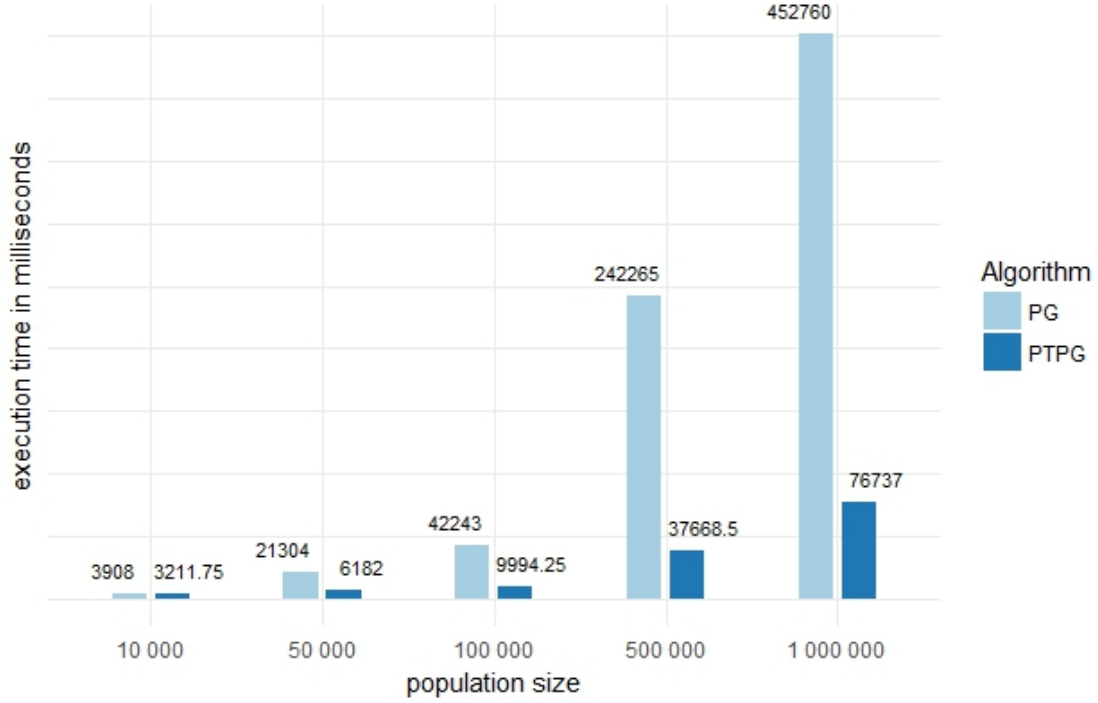


Figure 11: Execution time in milliseconds for PTPG and PG algorithms

and fulfils the assumption (2.3). Equation (A.5) arises in the context of Continuous Time Bayesian Networks (CTBNs), c.f. (Nodelman, 2007). Processes Ξ and Υ may correspond to hidden and observed nodes of a CTBN, respectively. Then the posterior distribution of Ξ describes “probabilistic inference” about the behaviour of the hidden nodes. Monte Carlo methods for CTBNs are subject of articles (Nodelman et al., 2002; Nodelman, 2007; Rao and Teh, 2013). Our algorithms based on Poisson resampling can also be used for CTBNs.

To conclude this section, note that discrete time models can be considered as a special case of continuous time models. Let $\Xi = (X_1, \dots, X_m)$ be a discrete time Markov chain (in general, inhomogeneous in time) with one-step transition kernels P_1, \dots, P_{m-1} . Using a convention explained earlier, let us express the initial distribution as $\mathbb{P}(X_1 \in dx_1) = P_0(x_0, dx_1)$ for a fictitious state x_0 and write $\mathbb{P}(X_t \in dx_t | X_{t-1} = x_{t-1}) = P_{t-1}(x_{t-1}, dx_t)$, for $t = 1, \dots, m$. Of course, Ξ can be identified with the continuous time process which is equal to X_t on the interval $[t-1, t[$. (To keep the notation consistent, put $t_{\min} = 0$, $t_{\max} = m-1$, $K(x_{t-1}, t-1; dx_t, \{t\}) = P_{t-1}(x_{t-1}, dx_t)$ and $T_t = t$ for $t = 1, \dots, m$.) The natural assumption about the process of observations in the discrete time setting is that $\Upsilon = (Y_1, \dots, Y_m)$, where Y_t depends only on *one* state X_t of the Markov chain. The likelihood is of the form $\ell_t(x_t) = \ell_t(y_t | x_t)$.

B Illustrative Examples

We provide two simple examples which illustrate the main idea behind our algorithms and the key elements of the proofs.

Why Poisson resampling works

The example presented in this subsection basically corresponds to a single “propagation” step of algorithm PTPF. Consider an importance sampling procedure with Poisson resampling. Let p be a probability density on space \mathcal{X} equipped with measure dx . The target density is

$$\pi(x) = \frac{p(x)w(x)}{z},$$

where w is a weight (importance) function and $z = \int_{\mathcal{X}} p(x)w(x)dx$. We interpret p as a prior distribution and w as the likelihood of observing y given x ($w(x) = \ell(y|x)$, where y is fixed). In this interpretation, π becomes the posterior distribution.

The sampling scheme is the following. Draw $N \sim \text{Poiss}(\lambda)$. If $N = 0$ then do nothing and put $\hat{Z} = 0$. If $N > 0$ then draw independently $X_1, \dots, X_N \sim p(\cdot)$. Put $\hat{Z} = \sum_{j=1}^N w(X_j)/\lambda$. It is obvious that $\mathbb{E}\hat{Z} = z$. Choose $S \in \{1 : N\}$ with probability

$$\mathbb{P}(S = s | N, X_1, \dots, X_N) = \frac{w(X_s)}{\sum_{j=1}^N w(X_j)}.$$

We say that the joint probability distribution of all the random variables generated in such a way is the *extended proposal*. It is denoted by ψ and given by

$$(B.1) \quad \psi(n, x_1, \dots, x_n, s) = e^{-\lambda} \frac{\lambda^n}{n!} \prod_{j=1}^n p(x_j) \frac{w(x_s)}{\sum_{j=1}^n w(x_j)}$$

for $n > 0$ and $\psi(0) = e^{-\lambda}$. Note that ψ is defined on the space $\{0\} \cup \bigcup_{n=1}^{\infty} \{n\} \times \mathcal{X}^n \times \{1 : n\}$.

Define the *extended target* probability distribution ϕ by

$$(B.2) \quad \phi(n, x_1, \dots, x_n, s) = e^{-\lambda} \frac{\lambda^n}{n!} \prod_{j=1}^n p(x_j) \frac{w(x_s)}{\lambda z}$$

for $n = 1, 2, \dots$ and $\phi(0) = 0$. Note that ϕ can be decomposed as follows:

$$(B.3) \quad \phi(n, x_1, \dots, x_n, s) = \underbrace{\frac{p(x_s)w(x_s)}{z}}_{\text{marginal}} \cdot \underbrace{\frac{1}{n} e^{-\lambda} \frac{\lambda^{n-1}}{(n-1)!} \prod_{j \neq s} p(x_j)}_{\text{conditional}}.$$

Formula (B.3) shows that ϕ is properly normalized and the marginal distribution of $X = X_S$ is exactly $\pi(\cdot)$. The conditional distribution of all the remaining variables can be obtained in the following way. The number of the other samples, $N - 1$, has the Poisson distribution. Once $N - 1$ is selected, we assign X label S chosen uniformly at random from the set $\{1 : N\}$, then draw $N - 1$ samples from $p(\cdot)$ and assign them labels $\{1 : N\} \setminus \{S\}$. If we start with $X \sim \pi(\cdot)$, then the conditional sampling scheme described above produces a configuration (N, X_1, \dots, X_N, S) such that $X = X_S$, and this configuration has the extended target distribution. From formula (B.2) it is clear that the conditional probability of S given N, X_1, \dots, X_N is proportional to $w(X_S)$. If we select new S' from this probability distribution then $X_{S'} \sim \pi(\cdot)$. The update X to $X_{S'}$ is just a single step of the *Particle Gibbs Sampler* (PGS) in our simplified example. We have thus verified that PGS preserves the target.

To see that the *Particle Independent Metropolis-Hastings* (PIMH) also preserves the target, it is enough to note that

$$\frac{\phi(n, x_1, \dots, x_n, s)}{\psi(n, x_1, \dots, x_n, s)} = \frac{\hat{z}}{z}, \quad \hat{z} = \sum_{j=1}^n w(x_j)/\lambda.$$

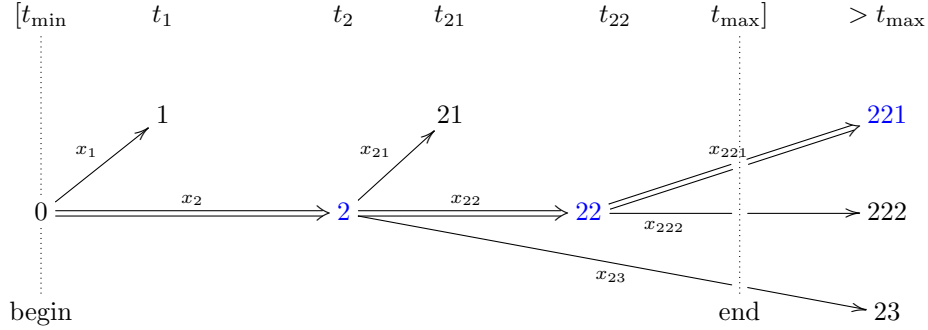
In our example, PIMH first generates a proposal $(X_{S^*}^*, \hat{Z}^*)$, obtained in a new run of the above-described (unconditional) sampling scheme. Then PIMH updates (X_S, \hat{Z}) to $(X_{S^*}^*, \hat{Z}^*)$ with probability $[\hat{Z}^*/\hat{Z}] \wedge 1$. We have verified that this is a valid Metropolis-Hastings update.

Similar arguments are used (in a much more complicated setting) to show that our main algorithms PTGS and PTMH are correct.

An example of Poisson Tree

The example presented here explains the basic relation between the extended target ψ and extended target ϕ . It also illustrates notation used in our paper.

For simplicity, assume that the process Ξ is *piece-wise constant*. Consequently, in the tree produced by PTPF, constant value x_i corresponds to the time interval $[t_{\text{pa}(i)}, t_i[$. Consider the tree depicted below. In our example we use a special way of labelling nodes with their full ancestor paths. The artificial root is 0.



Selected terminal node is 221 and the corresponding sample path is $x_2, x_{22}, x_{221}; t_2, t_{22}, t_{221}$ (nodes indicated in blue and edges with double arrows).

The *extended proposal* (probability of sampling the depicted configuration) in our example is

$$\begin{aligned}
 \psi(\mathcal{V}, \mathcal{E}, \mathbf{dx}, \mathbf{dt}, s = 221) = & \exp[-\lambda_0] (\lambda_0)^2 K(x_0, t_0; dx_1, dt_1) K(x_0, t_0; dx_2, dt_2) \\
 & \times \exp[-\lambda_1 w_1] \\
 & \times \exp[-\lambda_2 w_2] (\lambda_2 w_2)^3 K(x_2, t_2; dx_{21}, dt_{21}) K(x_2, t_2; dx_{22}, dt_{22}) \\
 & \quad K(x_2, t_2; dx_{23}, dt_{23}) \\
 & \times \exp[-\lambda_{21} w_{21}] \\
 & \times \exp[-\lambda_{22} w_{22}] (\lambda_{22} w_{22})^2 K(x_{22}, t_{22}; dx_{221}, dt_{221}) K(x_{22}, t_{22}; dx_{222}, dt_{222}) \\
 & \times \frac{1}{\hat{z}} \cdot \frac{w_{221}}{\lambda_0 \lambda_2 \lambda_{22}},
 \end{aligned}$$

where

$$\hat{z} = \frac{w_{221}}{\lambda_0 \lambda_2 \lambda_{22}} + \frac{w_{222}}{\lambda_0 \lambda_2 \lambda_{22}} + \frac{w_{23}}{\lambda_0 \lambda_2}.$$

The *extended target* is

$$\begin{aligned}
\phi(\mathcal{V}, \mathcal{E}, d\mathbf{x}, d\mathbf{t}, s = 221) &= \psi(\mathcal{V}, \mathcal{E}, d\mathbf{x}, d\mathbf{t}, s = 221) \frac{\hat{z}}{z} \\
&= \frac{1}{z} K(x_0, t_0; dx_2, dt_2) w_2 K(x_2, t_2; dx_{22}, dt_{22}) w_{22} K(x_{22}, t_{22}; dx_{221}, dt_{221}) w_{221} \\
&\times \exp[-\lambda_0] (\lambda_0)^1 K(x_0, t_0; dx_1, dt_1) \\
&\times \exp[-\lambda_1 w_1] \\
&\times \exp[-\lambda_2 w_2] (\lambda_2 w_2)^2 K(x_2, t_2; dx_{21}, dt_{21}) K(x_2, t_2; dx_{23}, dt_{23}) \\
&\times \exp[-\lambda_{21} w_{21}] \\
&\times \exp[-\lambda_{22} w_{22}] (\lambda_{22} w_{22})^1 K(x_{22}, t_{22}; dx_{222}, dt_{222}) \\
&= \pi(dx_2, dx_{22}, dx_{221}; dt_2, dt_{22}, dt_{221}) \\
&\times \psi_{\text{cond}}(\mathcal{V}, \mathcal{E}, d\mathbf{x}, d\mathbf{t} | x_2, x_{22}, x_{221}; t_2, t_{22}, t_{221}).
\end{aligned}$$

In the above formulae, terms indicated in blue correspond to the selected path. The second formula follows from the first one via rearrangement of blue terms.

The weights are given by

- $w_1 = \ell(x_1; t_0, t_1)$, $w_2 = \ell(x_2; t_0, t_2)$,
- $w_{21} = \ell(x_{21}; t_2, t_{21})$, $w_{22} = \ell(x_{22}; t_2, t_{22})$, $w_{23} = \ell(x_{23}; t_2, t_{23})$,
- $w_{221} = \ell(x_{221}; t_{22}, t_{221})$, $w_{222} = \ell(x_{221}; t_{22}, t_{221})$.

To illustrate our definition of the history, consider e.g. node 21. We have $\lambda_{21} = \mathbb{L}(\mathcal{H}(t_{21}))$, where $\mathcal{H}(t_{21}) = \{0; 1, 0 \rightarrow 1, x_1, t_1; 2, 0 \rightarrow 2, x_2, t_2; 21, 2 \rightarrow 21, x_{21}, t_{21}; 22, 2 \rightarrow 22, x_{22}, t_{22}; 23, 2 \rightarrow 23, x_{23}, t_{23}\}$.

Finally note that the equivalence class in our example contains $2 \cdot 3 \cdot 2$ trees which differ from the depicted one by different numbering of $\text{ch}(0)$, $\text{ch}(2)$ and $\text{ch}(22)$. This is why factors 2, 3, 2 are omitted in the Poisson probabilities in the formula for ψ .

C Proofs

We give proofs omitted in our paper.

Proof of Theorem 2

Define a sequence of nonnegative measurable functions f_0, f_1, \dots, f_m by backward induction as follows. Begin with $f_m(x_{1:m}) = \mathbb{1}(x_{1:m} \in \mathcal{D})$ and let

$$f_{t-1}(x_{1:t-1}) = \int_{\mathcal{X}} f_t(x_{1:t-1}, x_t) \ell_t(x_t) P_{t-1}(x_{t-1}, dx_t),$$

so that f_t is a function on \mathcal{X}^t . In agreement with our convention introduced in Section 2, the above equation extends also to $t = 1$ (f_0 is really a scalar, being formally “a function of the fictitious x_0 ”). Note that

$$f_0 = z\pi(\mathcal{D}).$$

Define also a sequence of nonnegative measurable functions h_0, h_1, \dots, h_m by backward induction. Let $h_m(x_m) = 1$ and

$$h_{t-1}(x) = \int_{\mathcal{X}} h_t(x_t) \ell_t(x_t) P_{t-1}(x, dx_t) + \frac{2}{\lambda_0} \|h_t \ell_t\|_{\infty},$$

so that h_t is a function on \mathcal{X} and, by convention, h_0 is a scalar.

Recall that $\mathcal{V}_t = \{j \in \mathcal{V} : T_j = t\}$ for $t = 1, \dots, m$. The main ingredient of the proof is the following inequality. For $t = 1, \dots, m$,

$$(C.1) \quad \mathbb{E} \frac{\sum_{j \in \mathcal{V}_t} W_j f_t(X_{\text{an}(j)})}{\sum_{j \in \mathcal{V}_t} W_j h_t(X_j)} \geq \mathbb{E} \frac{\sum_{i \in \mathcal{V}_{t-1}} W_i f_{t-1}(X_{\text{an}(i)})}{\sum_{i \in \mathcal{V}_{t-1}} W_i h_{t-1}(X_i)}.$$

Note that for $t = 1$ the RHS of this inequality reduces to f_0/h_0 (we again recall the convention about the fictitious state at $t = 0$, so we can put $\mathcal{V}_0 = \{0\}$ and $W_0 = 1$).

To prove (C.1) we first observe that sampling particles in \mathcal{V}_t can be equivalently done as follows.

- First we sample $N - 1 \sim \text{Pois}(\lambda_0)$ and create $N - 1$ particles in \mathcal{V}_t (note that $|\mathcal{V}_t| = N$, since we always have one particle in the conditioning path $x_{1:m}$; in accordance with the pseudo-code for cPTGS this particle corresponds to node labelled $j = t$).
- If $N - 1 = 0$ then $\mathcal{V}_t = \{t\}$. Otherwise, for every $j \in \mathcal{V}_t \setminus \{t\}$ we choose its parent with probability $\mathbb{P}(\text{pa}(j) = i) \propto W_i$. Then, of course, sample $X_j \sim P_{t-1}(X_i, \cdot)$.

Indeed, every node $i \in \mathcal{V}_{t-1} \setminus \{t-1\}$ has number of children equal to $N_i \sim \text{Pois}(\Lambda_{t-1} W_i)$ and for $i = t-1$ we have $N_i - 1 \sim \text{Pois}(\Lambda_{t-1} W_i)$, see (3.4). Our rule (5.1) entails $\Lambda_{t-1} \sum_{i \in \mathcal{V}_{t-1}} W_i = \lambda_0$. Consequently, $N - 1 = \sum_{i \in \mathcal{V}_{t-1}} N_i - 1 \sim \text{Pois}(\lambda_0)$, and our claim follows from the well-known property of the Poisson distribution.

We can say that conditionally, given N , propagation of $(t-1)$ th generation particles in cPTPF is identical as in the classical conditional PF with deterministic number of particles and with multinomial resampling. In particular, new particles of t th generation are conditionally independent, identically distributed. This fact will be used in the inequalities to follow.

To lighten notation write $\mathcal{H} = \mathcal{H}(t-1)$ for (the σ -field generated by) the history up to $t-1$ and $N = |\mathcal{V}_t|$. In the formula below we denote by j_0 an arbitrarily chosen node in $\mathcal{V}_t \setminus \{t\}$, if $|\mathcal{V}_t| > 1$. If $|\mathcal{V}_t| = N = 1$ then the expression involving (unspecified) j_0 is equal to 0. Analogous remark applies to $\sum_{j \in \mathcal{V}_t, j \neq j_0, j \neq t} [\dots]$. If $N \leq 2$ then the sum is “empty” and, by convention, equal to 0. In the third line below we use the Jensen inequality combined with the fact that the numerator and denominator are independent.

$$\begin{aligned} \mathbb{E} \left[\frac{\sum_{j \in \mathcal{V}_t} W_j f_t(X_{\text{an}(j)})}{\sum_{j \in \mathcal{V}_t} W_j h_t(X_j)} \middle| \mathcal{H}, N \right] &\geq \mathbb{E} \left[\frac{(N-1) W_{j_0} f_t(X_{\text{an}(j_0)})}{\sum_{j \in \mathcal{V}_t} W_j h_t(X_j)} \middle| \mathcal{H}, N \right] \\ &\geq \mathbb{E} \left[\frac{(N-1) W_{j_0} f_t(X_{\text{an}(j_0)})}{\sum_{j \in \mathcal{V}_t, j \neq j_0, j \neq t} W_j h_t(X_j) + 2\|\ell_t h_t\|_{\infty}} \middle| \mathcal{H}, N \right] \\ &\geq \frac{(N-1) \mathbb{E} [W_{j_0} f_t(X_{\text{an}(j_0)}) | \mathcal{H}, N]}{\mathbb{E} [\sum_{j \in \mathcal{V}_t, j \neq j_0, j \neq t} W_j h_t(X_j) | \mathcal{H}, N] + 2\|\ell_t h_t\|_{\infty}} \\ &= \frac{(N-1) \mathbb{E} [W_{j_0} f_t(X_{\text{an}(j_0)}) | \mathcal{H}, N]}{(N-2)_+ \mathbb{E} [W_j h_t(X_j) | \mathcal{H}, N] + 2\|\ell_t h_t\|_{\infty}}. \end{aligned}$$

Now note that

$$\begin{aligned}\mathbb{E} \left[W_{j_0} f_t(X_{\text{an}(j_0)}) \middle| \mathcal{H}, N \right] &= \sum_{i \in \mathcal{V}_{t-1}} \frac{W_i}{W^{(t-1)}} \int \ell_t(x) f_t(X_{\text{an}(i)}, x) P_{t-1}(X_i, dx) \\ &= \sum_{i \in \mathcal{V}_{t-1}} \frac{W_i}{W^{(t-1)}} f_{t-1}(X_{\text{an}(i)})\end{aligned}$$

and, analogously,

$$\begin{aligned}\mathbb{E} \left[W_j h_t(X_j) \middle| \mathcal{H}, N \right] &= \sum_{i \in \mathcal{V}_{t-1}} \frac{W_i}{W^{(t-1)}} \int \ell_t(x) h_t(X_i, x) P_{t-1}(X_i, dx) \\ &= \sum_{i \in \mathcal{V}_{t-1}} \frac{W_i}{W^{(t-1)}} \tilde{h}_{t-1}(X_i),\end{aligned}$$

where $W^{(t-1)} = \sum_{i \in \mathcal{V}_{t-1}} W_i$ and $\tilde{h}_{t-1} = h_{t-1} - \frac{2}{\lambda_0} \|\ell_t h_t\|_\infty$. Consequently,

$$\mathbb{E} \left[\frac{\sum_{j \in \mathcal{V}_t} W_j f_t(X_{\text{an}(j)})}{\sum_{j \in \mathcal{V}_t} W_j h_t(X_j)} \middle| \mathcal{H}, N \right] \geq \frac{(N-1) \sum_{i \in \mathcal{V}_{t-1}} W_i f_{t-1}(X_{\text{an}(i)})}{(N-2)_+ \sum_{i \in \mathcal{V}_{t-1}} W_i \tilde{h}_{t-1}(X_i) + 2 \sum_{i \in \mathcal{V}_{t-1}} W_i \|\ell_t h_t\|_\infty}.$$

Dropping N from the condition we obtain, by Jensen inequality,

$$\begin{aligned}&\mathbb{E} \left[\frac{\sum_{j \in \mathcal{V}_t} W_j f_t(X_{\text{an}(j)})}{\sum_{j \in \mathcal{V}_t} W_j h_t(X_j)} \middle| \mathcal{H} \right] \\ &\geq \sum_{n=1}^{\infty} e^{-\lambda_0} \frac{\lambda_0^{n-1}}{(n-1)!} \cdot \frac{(n-1) \sum_{i \in \mathcal{V}_{t-1}} W_i f_{t-1}(X_{\text{an}(i)})}{(n-2)_+ \sum_{i \in \mathcal{V}_{t-1}} W_i \tilde{h}_{t-1}(X_i) + 2 \sum_{i \in \mathcal{V}_{t-1}} W_i \|\ell_t h_t\|_\infty} \\ &= \lambda_0 \sum_{n=2}^{\infty} e^{-\lambda_0} \frac{\lambda_0^{n-2}}{(n-2)!} \cdot \frac{\sum_{i \in \mathcal{V}_{t-1}} W_i f_{t-1}(X_{\text{an}(i)})}{(n-2) \sum_{i \in \mathcal{V}_{t-1}} W_i \tilde{h}_{t-1}(X_i) + 2 \sum_{i \in \mathcal{V}_{t-1}} W_i \|\ell_t h_t\|_\infty} \\ &\geq \frac{\lambda_0 \sum_{i \in \mathcal{V}_{t-1}} W_i f_{t-1}(X_{\text{an}(i)})}{\lambda_0 \sum_{i \in \mathcal{V}_{t-1}} W_i \tilde{h}_{t-1}(X_i) + 2 \sum_{i \in \mathcal{V}_{t-1}} W_i \|\ell_t h_t\|_\infty} \\ &= \frac{\sum_{i \in \mathcal{V}_{t-1}} W_i f_{t-1}(X_{\text{an}(i)})}{\sum_{i \in \mathcal{V}_{t-1}} W_i h_{t-1}(X_i)}.\end{aligned}$$

It is now enough to apply \mathbb{E} to both sides of the above inequality to obtain (C.1).

The rest of the proof is easy. By definition of PTGS, using the form of functions f_t and (C.1) we obtain

$$\begin{aligned}\mathbb{P}(X'_{1:m} \in \mathcal{D} | X_{1:m} = x_{1:m}) &= \mathbb{E} \frac{\sum_{i \in \mathcal{V}_m} W_i \mathbb{1}(X_{\text{an}(i)} \in \mathcal{D})}{\sum_{i \in \mathcal{V}_m} W_i} \\ &= \mathbb{E} \frac{\sum_{i \in \mathcal{V}_m} W_i f_m(X_{\text{an}(i)})}{\sum_{i \in \mathcal{V}_m} W_i h_m(X_i)} \\ &\geq \mathbb{E} \frac{f_0}{h_0} = \frac{z\pi(\mathcal{D})}{h_0},\end{aligned}$$

which concludes the proof.

Proof of Theorem 3

Proof. As in the proof of Theorem 4.2, we note that the configuration obtained by cPTPF has the extended target distribution ϕ , provided that at the input $X_{1:m} \sim \pi$. We are to show that $(\mathcal{V}, \mathcal{E}, \mathbf{X}, S) \sim \phi$ implies

$(\mathcal{V}, \mathcal{E}', \mathbf{X}, S) \sim \phi$. PTGAS-dt consists of a series of samplings from full conditional distributions of single arrows, $\phi(i' \rightarrow j | \mathcal{V}, \mathcal{E} \setminus \{i \rightarrow j\}, \mathbf{X}, S)$. Formulae (3.3) and (3.2) allow us to compute these conditional distributions. Crucial points are the following. The weights do not depend on the arrows. The intensity parameters do not depend on the arrows either, because they are given by (5.1). The same is true for the estimate \hat{z} , because $\hat{z} = \sum_{s \in \mathcal{V}_{\text{end}}} w_s / (\prod_{g=0}^{m-1} \lambda_g)$. Consequently, if $\mathcal{V}, \mathbf{x}, s$ are fixed and we denote $\mathcal{E}' = (\mathcal{E} \setminus \{i \rightarrow j\}) \cup \{i' \rightarrow j\}$ then we have

$$\frac{\phi(\mathcal{V}, \mathcal{E}', \mathbf{x}, s)}{\phi(\mathcal{V}, \mathcal{E}, \mathbf{x}, s)} = \frac{w_{i'} p_{t-1}(x_{i'}, x_j)}{w_i p_{t-1}(x_i, x_j)}.$$

Therefore, $\phi(\mathcal{E}' | \mathcal{V}, \mathcal{E} \setminus \{i \rightarrow j\}, \mathbf{x}, s) \propto w_{i'} p_{t-1}(x_{i'}, x_j)$. We have shown that t th small step in PTGAS-dt, that is sampling new edge $i' \rightarrow j$, preserves ϕ . \square

Proof of Theorem 4

Similarly as in the proof of Theorem 5.3 it is enough to consider a small step of sampling an arrow $i' \rightarrow j$. We are to show that the move from $i \rightarrow j$ to $i' \rightarrow j$ preserves ϕ . Write $\mathcal{E}' := (\mathcal{E} \setminus \{i \rightarrow j\}) \cup \{i' \rightarrow j\}$. Below we use lower case letters to denote values of random variables appearing in (5.4) and in pseudo-code PTGAS-ct. Let us recall that ϕ is given by (3.3):

$$\phi(\mathcal{V}, \mathcal{E}, d\mathbf{x}, d\mathbf{t}, s) = \frac{1}{z} \prod_{k \in \mathcal{V} \setminus \mathcal{V}_{\text{end}}} \exp[-\lambda_k w_k] (\lambda_k w_k)^{|\text{ch}(k)|} \prod_{l \in \text{ch}(k)} k(x_k, t_k; x_l, t_l) dx_l dt_l \frac{w_s}{c_{\text{pa}(s)}}.$$

We claim that the following equality holds

$$(C.2) \quad \frac{\phi(\mathcal{V}, \mathcal{E}', d\mathbf{x}, d\mathbf{t}, s)}{\phi(\mathcal{V}, \mathcal{E}, d\mathbf{x}, d\mathbf{t}, s)} = \frac{w_{i'} w_{i \rightarrow j} \cdot k(x_{i'}, t_{i'}; x_j, t_j)}{c_{\text{pa}(i')}} \cdot \frac{c_{\text{pa}(i)}}{w_i w_{i \rightarrow j} \cdot k(x_i, t_i; x_j, t_j)},$$

provided that $j \in \mathcal{F}^r \cap \text{an}(S)$ and $i, i' \in \mathcal{F}^p$ with $p < r-1$. The correctness of PTGAS-ct will follow, because (C.2) shows that the probability of sampling an arrow $i' \rightarrow j$ is proportional to $\phi(\mathcal{E}' | \mathcal{V}, \mathcal{E} \setminus \{i \rightarrow j\}, \mathbf{x}, \mathbf{t}, s)$ in “strata” corresponding to strips \mathcal{F}^p .

We are left with the task of proving (C.2). Begin with the following simple observations:

- For any q sets of nodes $\mathcal{F}^q, \mathcal{G}^q$ and \mathcal{F}_o^q remain unchanged if $i \rightarrow j$ is replaced by $i' \rightarrow j$ (because i and i' belong to the same strip).
- Since $j \in \mathcal{G}^{r-1}$ we ensure that w_j^r remains unchanged. The same is true for all descendants of j and i' . Consequently for any node l , its Poisson parameter $w_l \lambda_l$ remains unchanged.
- Quotient $k(x_{i'}, t_{i'}; dx_j, dt_j) / k(x_i, t_i; dx_j, dt_j)$ appears in (C.2), for the obvious reason.
- Expression $\lambda_{i'} w_{i'} / \lambda_i w_i$ appears in the ratio, because $|\text{ch}(i')|$ is increased by one and $|\text{ch}(i)|$ is decreased by one.

Apart from the items listed above, we have to consider changes in the expression $c_{\text{pa}(s)} = \prod_{k \in \text{an}(s) \setminus \{s\}} \lambda_k$ (we assume that $j \in \text{an}(s)$). Let us use the notations $c_{\text{pa}(s)}$ and $c'_{\text{pa}(s)}$ for the quantities before and after replacing $i \rightarrow j$ by $i' \rightarrow j$.

Note that $c_{\text{pa}(s)}$ can be factorised into $c_{\text{pa}(i)} \lambda_i \lambda_j L$ where L depends only on descendants of j and consequently cancels out in the ratio $c_{\text{pa}(s)} / c'_{\text{pa}(s)}$. According to (5.4),

$$\lambda_j = \frac{1}{w_j} \frac{w_j^r}{w_o^r} b(\lambda_0 - |\mathcal{G}^r|),$$

In this expression only w_j may change if we replace $i \rightarrow j$ by $i' \rightarrow j$ ($w_j = w_{i \rightarrow j}$ is replaced by $w_{i' \rightarrow j}$). This fact is easy to see from the preceding discussion. As a result,

$$\frac{c_{\text{pa}(s)}}{c'_{\text{pa}(s)}} = \frac{c_{\text{pa}(i)} \lambda_i w_{i' \rightarrow j}}{c_{\text{pa}(i')} \lambda_{i'} w_{i \rightarrow j}}.$$

Combining everything together we arrive at

$$\frac{\phi(\mathcal{V}, \mathcal{E}', \mathbf{dx}, \mathbf{dt}, s)}{\phi(\mathcal{V}, \mathcal{E}, \mathbf{dx}, \mathbf{dt}, s)} = \frac{k(x_{i'}, t_{i'}; \mathbf{dx}_j, \mathbf{dt}_j)}{k(x_i, t_i; \mathbf{dx}_j, \mathbf{dt}_j)} \cdot \frac{\lambda_{i'} w_{i'}}{\lambda_i w_i} \cdot \frac{c_{\text{pa}(i)} \lambda_i w_{i' \rightarrow j}}{c_{\text{pa}(i')} \lambda_{i'} w_{i \rightarrow j}}.$$

We have verified (C.2) and thus finished the proof.

D Comparison of parallel implementations

In the literature there exist several approaches to construction of enhanced parallel SMC algorithms. One of those includes reducing overhead introduced by cumulative weight normalisation. This has been a focus of (L.M. Murray, 2015) – to this end they employ methods based on Metropolis and rejection resampling to bypass difficulties caused by vector reduction step. Authors’ scheme enables more efficient GPU implementations, by far exceeding PTPF’s capabilities in this area, though the amount of data shared between threads is still equal to $\mathcal{O}(N)$ in a worst case scenario.

Both algorithms do not avoid the necessity of machine-wide synchronisation after each propagation step – in case of PTPF all threads must receive each other’s normalizing constants, in case of (L.M. Murray, 2015) approach all threads must receive unnormalized particles’ weights.

PTPF bears a strong resemblance to a scheme introduced in (Paige et al., 2014b) – ”the Particle Cascade”. Authors’ approach enables asynchronous particles propagation, in effect getting rid of crude global synchronisation after each step (but synchronisation is still present implicitly because strong ordering on the times of particles reaching next propagation step must be imposed) and analogously to PTPF considerable decrease of amount of data which must be shared between threads.

PC’s unique scheme encourages feeding new particles into system continuously – to progressively improve results. However, fluctuations in number of alive particles are harder to control. In comparison in the case of PTPF we have found those alterations to be negligible (see Figure 9) – a result of more restrictive synchronisation.

References

- C. Andrieu, A. Doucet, and R. Holenstein. Particle markov chain monte carlo methods. *Journal of the Royal Statistical Society: Series B (Statistical Methodology)*, 72(3):269–342, jun 2010. doi: 10.1111/j.1467-9868.2009.00736.x.
- A. Bouchard-Côté, S. Sankararaman, and M. I. Jordan. Phylogenetic inference via sequential monte carlo. *Systematic Biology*, 61(4):579–593, jan 2012. doi: 10.1093/sysbio/syr131.
- F. Cérou, P. D. Moral, T. Furon, and A. Guyader. Sequential monte carlo for rare event estimation. *Statistics and Computing*, 22(3):795–808, apr 2011. doi: 10.1007/s11222-011-9231-6.
- M. H. A. Davis. Piecewise-deterministic Markov processes: a general class of nondiffusion stochastic models. *J. Roy. Statist. Soc. Ser. B*, 46(3):353–388, 1984. ISSN 0035-9246. With discussion.

- A. Doucet, N. Freitas, and N. Gordon, editors. *Sequential Monte Carlo Methods in Practice*. Springer New York, 2001. doi: 10.1007/978-1-4757-3437-9.
- A. Finke, A. M. Johansen, and D. Spanò. Static-parameter estimation in piecewise deterministic processes using particle gibbs samplers. *Annals of the Institute of Statistical Mathematics*, 66(3):577–609, mar 2014. doi: 10.1007/s10463-014-0455-z.
- A. Golightly and D. J. Wilkinson. Bayesian parameter inference for stochastic biochemical network models using particle markov chain monte carlo. *Interface Focus*, 1(6):807–820, sep 2011. doi: 10.1098/rsfs.2011.0047.
- N. Gordon, D. Salmond, and A. Smith. Novel approach to nonlinear/non-gaussian bayesian state estimation. *IEE Proceedings F Radar and Signal Processing*, 140(2):107, 1993. doi: 10.1049/ip-f-2.1993.0015.
- S. Kim, N. Shepherd, and S. Chib. Stochastic volatility: Likelihood inference and comparison with ARCH models. *Review of Economic Studies*, 65(3):361–393, jul 1998. doi: 10.1111/1467-937x.00050.
- F. Lindsten, M. I. Jordan, and T. B. Schön. Particle gibbs with ancestor sampling. *Journal of Machine Learning Research*, 15:2145–2184, 2014.
- F. Lindsten, R. Douc, and E. Moulines. Uniform ergodicity of the particle Gibbs sampler. *Scand. J. Stat.*, 42(3):775–797, 2015. ISSN 0303-6898. doi: 10.1111/sjso.12136.
- P. J. L.M. Murray, A. Lee. Parallel resampling in the particle filter. *Journal of Computational and Graphical Statistics*, 25(3), 2015.
- P. D. Moral, A. Doucet, and A. Jasra. Sequential monte carlo samplers. *Journal of the Royal Statistical Society: Series B (Statistical Methodology)*, 68(3):411–436, jun 2006. doi: 10.1111/j.1467-9868.2006.00553.x.
- L. M. Murray, A. Lee, and P. E. Jacob. Parallel resampling in the particle filter. *Journal of Computational and Graphical Statistics*, 25(3):789–805, jul 2016. doi: 10.1080/10618600.2015.1062015.
- C. A. Naesseth, F. Lindsten, and T. B. Schön. Sequential monte carlo for graphical models. In *Advances in Neural Information Processing Systems*, pages 1862–1870, 2014.
- U. Nodelman. *Continuous Time Bayesian Networks*. PhD thesis, Department of Computer Science, Stanford University, 2007.
- U. Nodelman, C. R. Shelton, and D. Koller. Continuous time bayesian networks. In *Proceedings of the Eighteenth conference on Uncertainty in artificial intelligence*, pages 378–387, 2002.
- B. Paige, F. Wood, A. Doucet, and Y. W. Teh. Asynchronous anytime sequential monte carlo. In Z. Ghahramani, M. Welling, C. Cortes, N. D. Lawrence, and K. Q. Weinberger, editors, *Advances in Neural Information Processing Systems 27*, pages 3410–3418. Curran Associates, Inc., 2014a.
- B. Paige, F. Wood, A. Doucet, and Y. W. Teh. Asynchronous anytime sequential monte carlo. pages 3410–3418, 2014b.
- V. Rao and Y. W. Teh. Fast MCMC sampling for Markov jump processes and extensions. *Journal of Machine Learning Research*, 14:3207–3232, 2013.
- R. Rudnicki and M. Tyran-Kamińska. *Piecewise Deterministic Processes in Biological Models*. Springer International Publishing, 2017. doi: 10.1007/978-3-319-61295-9.
- C. Schfer and N. Chopin. Sequential monte carlo on large binary sampling spaces. *Statistics and Computing*, 23(2):163–184, nov 2011. doi: 10.1007/s11222-011-9299-z.
- N. Whiteley, A. M. Johansen, and S. Godsill. Monte carlo filtering of piecewise deterministic processes. *Journal of Computational and Graphical Statistics*, 20(1):119–139, jan 2011. doi: 10.1198/jcgs.2009.08052.